AN ABSTRACT OF THE THESIS OF

HELEN ROSE DICKINSON for the DOCTOR OF PHILOSOPHY
(Name) (Degree)

in BIOCHEMISTRY AND BIOPHYSICS presented on April 11, 1972
(Major) (Date)

Title: VACUUM ULTRAVIOLET ABSORPTION STUDIES OF MODEL SUGAR COMPOUNDS

Abstract approved Redacted for privacy
W. Curtis Johnson

Vacuum ultraviolet absorption spectra of 13 model sugar compounds were measured in the energy range of 50 to 80 kK. The model sugars included three simple alcohols, four simple ethers, four cyclic alcohol-ether compounds, and two dioxanes. All spectra show transition bands in the energy region 50 to 65 kK.

When the model sugar spectra were compared to those for similar hydrocarbons, it was shown that the low energy transitions depend on the presence of the oxygen atom within the molecule. The question arose whether these transitions were due to $\sigma - \sigma^*$ transitions from CO or OH bonds or from nonbonding electrons on the oxygen. This was resolved by an independent systems calculation of the $\sigma - \sigma^*$ transitions for several of the model sugar compounds. The isolated bond transition energies for the series of bonds CH, OH, NH and

CC, CN, CO and CF were calculated both by the extended Huckel method and by the complete neglect of differential overlap (CNDO) method. Five separate calculations were performed including one completely empirical CNDO calculation. Experimental results for hydrocarbons and fluorocarbons indicated that the completely empirical method was the best approximation. The results of an independent systems calculation for the model sugar compounds showed that the low energy transitions were not $\sigma - \sigma^*$ transitions. Therefore we concluded that they must be nonbonding oxygen transitions.

The spectra of simple alcohols and ethers were then combined to predict spectra of the more complex model sugars and of glucose.

Vacuum Ultraviolet Absorption Studies of Model Sugar Compounds

by

Helen Rose Dickinson

A THESIS

submitted to

Oregon State University

in partial fulfillment of
the requirements for the
degree of

Doctor of Philosophy

June 1972

APPROVED:

Redacted for privacy

Assistant Professor of Biochemistry and Biophysics

in charge of major

Redacted for privacy

Acting Chairman of Department of Biochemistry and Biophysics

Redacted for privacy

Dean of Graduate School

Date thesis is presented April 11, 1972

Typed by Clover Redfern for Helen Rose Dickinson

ACKNOWLEDGMENTS

I wish to express appreciation to Professor W. Curtis Johnson for guidance and encouragement throughout the course of this research.

I would also like to thank Professors McDonald and Reed for advice concerning organic syntheses and analysis.

My thanks go to the U.S. Public Health Service for financial support.

TABLE OF CONTENTS

LIST OF FIGURES

LIST OF TABLES

VACUUM ULTRAVIOLET STUDIES OF MODEL SUGAR COMPOUNDS

INTRODUCTION

Carbohydrates are vital in many aspects of biology. They are of major importance in cell wall structure of plants and bacteria, and in the metabolism of all living things. Medically, they are gaining significance in the study of immunology.

Since carbohydrates are important in biology, we would like to understand more about their conformations, especially in polysaccharides. One goal of this laboratory is to use the techniques of vacuum ultraviolet spectroscopy to elucidate the structure of sugar monomers, oligomers, and polymers.

Before this can be accomplished, much must be learned about the electronic spectra of simple sugars. Vapor phase absorption spectroscopy of model sugar compounds gives information about where the transition bands lie. A second approach, circular dichroism of the same transition bands, tells about the conformation of the asymmetric sugars. It is not technically possible to take spectra of actual sugars below the cut-off point of water at this time. Some less complex molecules such as tetrahydrofuran and tetrahydropyran and simple alcohols can easily be studied in the vapor phase. In choosing our model compounds we assume that a sugar such as hexose may be

represented as a cyclic ether plus four OH groups and one CH_2OH group as shown below.

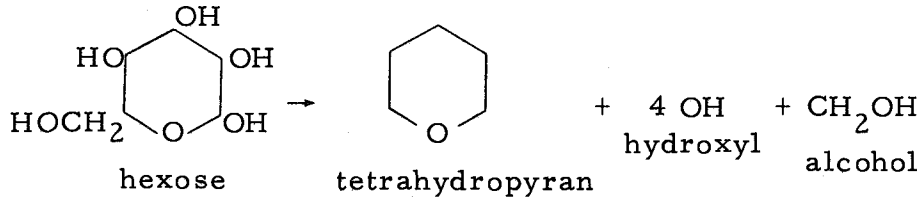

We recognize that this model is not quite complete. The hexose can exist both as a ring structure and as an open chain, since it is an aldol.

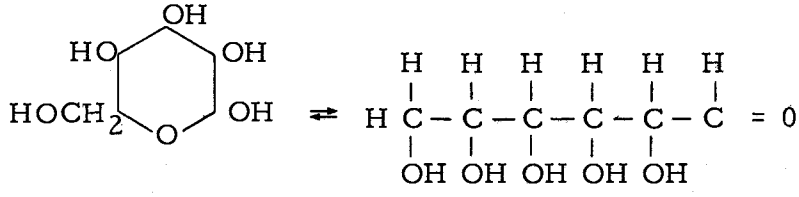

Thus, we have included an aldol in this study.

Spectra of the simple cyclic ether compounds tetrahydrofuran, tetrahydropyran and 1,4-dioxane were taken in the early 1950's by Pickett et al. (32) and by Hernandez (14, 15) who added 1,3-dioxane to the series. Harrison and Price (11) recorded spectra of diethyl, dimethyl and divinyl ethers. The two saturated ethers, dimethyl and diethyl ether, were later studied by Hernandez (12, 13). Spectra of the alcohols, methanol, ethanol, 1-propanol and 2-propanol, were recorded by Harrison et al. (10). Most of the spectra were limited by the available technique to the energy region below 65 kK.

(1 kK = 1000 cm^{-1} is the energy unit used in this work.) Spectra of dimethyl ether, diethyl ether, ethanol and methanol were later repeated and extended to 80 kK by Holden and subsequently interpreted by Edwards (5, pages 30-40). In the present work, I have repeated spectra of some of these compounds for internal consistency, extended other spectra, and added a number of new spectra of some cyclic ethers with alcohol groups attached.

These compounds all show a number of electronic transitions beginning at about 51 kK and continuing to higher energies. We proved that the bands at energies below 67 kK can be assigned to transitions in which the electron originates from a nonbonding orbital on the oxygen atom.

Initial evidence that the transitions are related to the oxygen atom comes from the study of the spectra of simple hydrocarbons by Raymonda (38), in which there is no absorbance below 65 kK. The molecular oxygen atoms have both bonding electrons (called σ) and nonbonding electrons (called n). Both can be excited by an antibonding state (called σ^*). It is not possible to measure pure $\sigma - \sigma^*$ transitions for CO or OH bonds experimentally. To establish that these transitions do not contribute to the low energy part of each spectrum, independent systems calculations were carried out to produce theoretical $\sigma - \sigma^*$ spectra for our saturated oxygen containing model compounds.

The unperturbed bond transition energies of CH, CC, CO and OH are needed for an independent systems calculation. The energies of a series of bonds were calculated by the extended Huckel molecular orbital method of Hoffmann (17), and also by the method of antisymmetrized products of molecular orbitals with complete neglect of differential overlap as developed by Pople et al (34, 35, 36). These calculations gave a variety of results, but the energy trends were consistent. Independent systems calculations gave profiles of the spectra of the compounds without nonbonding transitions.

We show that the bands having energies below 67 kK can not be $\sigma - \sigma^*$ transitions, and thus must be due to nonbonding electrons. Then we show that in tetrahydropyran-2-methanol and in 3-hydroxytetrahydrofuran, the low energy bands can be predicted from those of related simple alcohols and ethers. The transition bands of the alcohol, ether and hydrocarbon parts were combined graphically to produce the spectra of sugar analogs.

Two appendices are included. The first is a listing of the Fortran IV program used in the independent systems calculations. Though the first part was written by the author, the subroutine EIGVV was by M.S. Itzkowitz. Appendix II is a paper by H.R. Dickinson and W.C. Johnson which was published in Applied Optics (March 1971) entitled "Fluorocarbons as Solvents for Vacuum Ultraviolet."

EXPERIMENTAL

Apparatus

The Vacuum Line

The vacuum line was designed by W. C. Johnson and constructed by Arthur Vallier and Mario Boschetto (see Figure 1). It was used both for removing dissolved air from the sample and for introducing the sample into the light path of the spectrophotometer. Samples were stored in two-piece glass vessels joined by ground glass and sealed with a teflon stopcock. When these were joined to the entries of the vacuum line the sample could be released into the system. Sometimes calibrated spheres were used to contain a known amount of vapor for injection into the system. All the joints were greased with 'Spectrovac' low pressure stopcock grease from Robert Austin (Box 374E Pasadena, California). The stopcocks were all teflon vacuum valves from Kontes.

According to Beer's law, the absorbance (A) of a compound at a particular wavelength (λ) depends on the concentration (c) of the compound and the path length of the cell (ℓ). The extinction coefficient of the compound is a characteristic which may be determined from these factors.

$$\epsilon(\lambda) = \frac{A(\lambda)}{c\ell} \qquad (1)$$

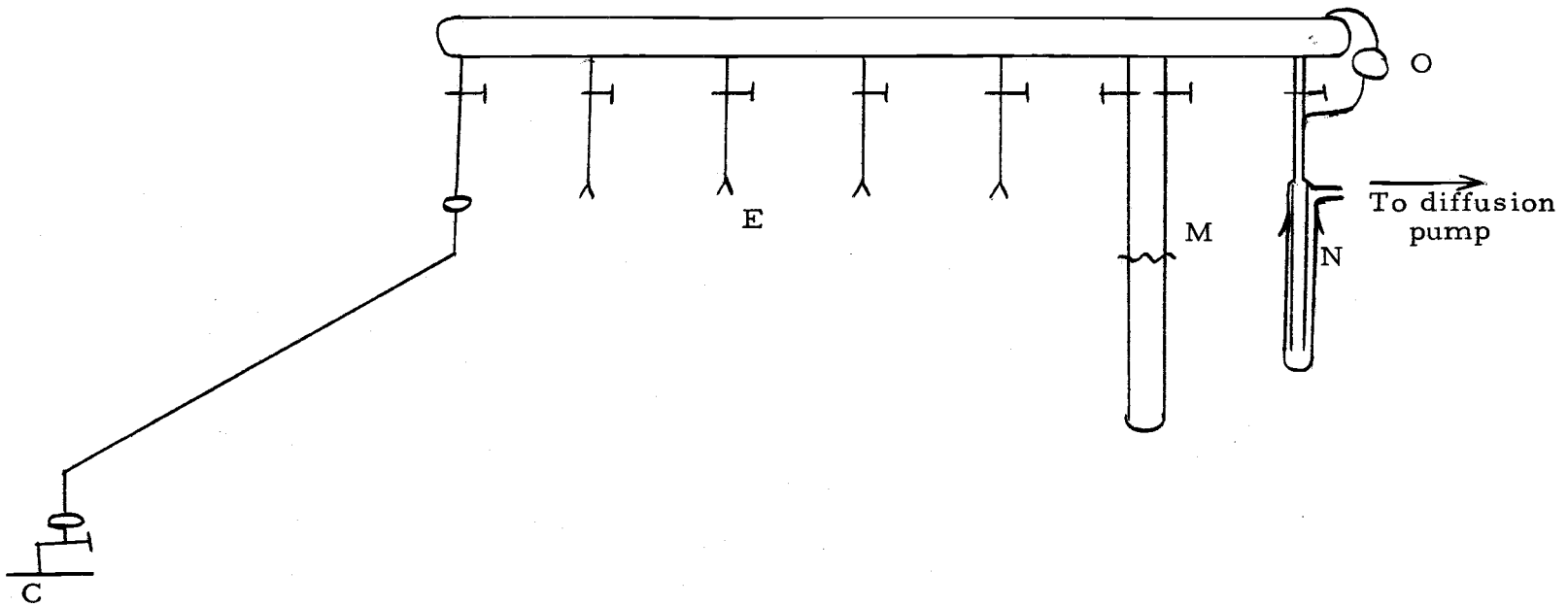

Figure 1. Diagram of the vacuum line.

C Cell
E Entries
M U tube mercury manometer
N Liquid nitrogen trap
O Oil gauge (micrometric manometer)

The three sample cells through which the spectra were taken had path lengths of 100, 10 and 1 mm. Since we used vapors at very low pressures, the perfect gas law may be used for the calculation of the concentrations.

$$c = \frac{n}{V} = \frac{P}{RT} \qquad (2)$$

n = Number of moles

V = Volume

P = Pressure

T = Temperature (absolute)

R = Gas constant (.082 liter atmospheres/degree mole)

Thus, it was very important to know the exact pressure of the sample. We needed pressure gauges that would be independent of the sample involved, since it would be impossible to calibrate a gauge for most of the compounds.

There are now three different pressure gauges which are attached directly to the vacuum line. These gauges were obtained in the same sequence as they are listed below. The measurement of the 13 spectra took about 18 months. Most of the spectra had already been measured by the time the most sophisticated gauge was obtained. A few samples were repeated on this gauge to show that the results were consistent.

The U tube mercury manometer is simply a U-shaped glass tube

one-half filled with mercury. With one side of the tube sealed and evacuated, the other side was exposed to the pressure from the sample. This caused the mercury level on the exposed side to be depressed. The change in mercury level was a direct measurement of the pressure, which was read with a cathetometer (Gairtner Scientific Company). Since it was difficult to keep the mercury in this gauge clean, it was not accurate for very low pressure measurements. With pressures between 5 and 15 mm Hg, the variation in the measured extinction coefficient was about 5%.

A more accurate micrometric manometer was obtained from Roger Gilmont Instruments, Inc. This gauge worked on the same principle as the U-tube mercury manometer but was made much more accurate by the use of dibutyl phthalate as manometer fluid. The oil was chosen first because it has a much lower density than mercury (1.04 g cm^{-3} for dibutyl phthalate as compared to 13.6 g cm^{-3} for mercury). The second reason for choosing dibutyl phthalate was that its vapor pressure is very low. This system measured pressures with an accuracy of 10^{-4} mm Hg.

There were, however, disadvantages to using this gauge, too. All our samples were soluble in the oil, so a vacuum would pull the molecules through the oil. The low pressure side had to be evacuated constantly. To maintain a constant pressure in the vacuum line it was necessary to leave the sample tube open to the system to replace

material being pumped away. The vapor pressure of the sample was controlled by keeping it in a cold bath as described below. Another effect of the sample-oil solubility was that all the sample in the oil had to be removed before an experiment could be done with a different compound.

The MKS Baratron Type 144 Series Pressure Meter is a capacitance manometer purchased from MKS Instruments, Inc. Its range is 30 to 3×10^{-3} mm Hg full scale for a difference between two chambers. We used the tank for the zero pressure in the reference chamber. The pressure in this case was read directly from a meter. The reading could be taken very quickly and accurately.

Cold Baths

It is possible to control the vapor pressure of a sample by keeping the sample in a cold bath at a constant temperature. The cold baths were actually certain organic compounds with liquid in equilibrium with their solids. Theoretically, the absorbance of the sample should have remained constant as long as there was both solid and liquid present in the bath. However, the actual measured absorbance at a particular wavelength was found to vary from 10 to 20% over a period of 30 minutes. Spectra taken without the cold bath in a closed system were usually more constant.

Windows

Windows were obtained from several sources at first. Some of the LiF windows polished for UV from Harshaw were only 0.6 absorbance units more opaque at 86 kK than at 50 kK. These were used exclusively in the beginning, but were abandoned because they develop color centers and because they are hygroscopic and become useless sitting around in the air. Eventually we changed to MgF_2 windows (Frank Cooke Inc., 59 Summer Street, North Brookfield, Mass. 01535). These are only transparent to 80 kK.

The Spectrophotometer

The spectra were all taken on a 1 meter grating vacuum ultraviolet spectrophotometer manufactured by McPherson Instrument Corp. The light source is a McPherson model 630 Hinteregger type discharge lamp. The capillary diameter has been reduced from 6 mm to 2.5 mm. The H_2 gas was bled through the lamp very slowly at a pressure of 1 mm. The McPherson model 730 dc power supply was used at 250 mA and about 1500 volts to run the source. The source is separated from the tank of the spectrophotometer by a MgF_2 window.

The monochromator is a McPherson model 225 equipped with a concave Bausch and Lomb tripartite grating ruled with 600 lines/mm. It is blazed at 1500 Å per mm and gives a dispersion of 16 Å per mm.

The chamber of the monochromator was maintained at a pressure of less than 10^{-5} torr. The entrance and exit slits were both set at a height of 4 mm and a width of 100 microns during the measurement of these spectra.

The spectra were measured through a double beam chamber (McPherson model 665) equipped with an oscillating mirror, a sample mount and a reference mount. On the sample side we used one of the standard cells supplied with two MgF_2 windows with two similar windows in the reference side as a blank. The vacuum ultraviolet light beam was converted to near visible by sodium salicylate coated windows in front of two end-on photomultiplier electron tubes (EMI type 9635B). The high voltage across the photomultiplier electron tubes was adjusted so that the current from either tube was in the range of 10^{-5} to 10^{-7} amperes over the wavelength range to be scanned. This usually amounted to 700 to 1000 volts.

The photomultiplier electron tube signal was converted to absorbance units by a McPherson model 782 logarithmic ratiometer and recorded on a Minneapolis-Honeywell recorder (Brown Instrument Division, Elektronic model 153x18).

Techniques

Source and Treatment of Chemicals

The chemicals used as samples are listed in Table 1 with structure, name, source and treatment. All of these were analyzed in some way. The most convenient method was gas-liquid chromatography (GLC). This worked well with chemicals whose boiling points were 100°C or greater. We were equipped with a Varian Aerograph by Wilkins (Model-A-90-P). We used a 6 feet by 1/4 inch copper column with 5% DEGS (diatomaceous earth glycol succinate) and 0.05% Igepal (nonyl phenoxy polyethylene ethanol) on 100/120 mesh Chromasorb G, acid washed and DMCS (dimethyl chloro silane) treated. We used helium as a carrier gas with a flow rate of about 20 ml per minute. The column temperature was maintained low enough so that the major peak took about 20 to 30 minutes to come off. The samples were injected neat, that is, with no carrier solvent. When samples of 2 µl showed only a major peak, they were considered to be pure. Compounds which showed minor peaks were distilled on the chromatography column. To accomplish this, lots of 70 to 90 µl were injected into the column and the major peak was collected as the recorder (Speedomax 8, Leeds Northrup Co.) showed it coming off the column. To get enough material for a spectrum, this procedure was repeated three times. This yielded a total of two or three drops.

Table 1. Source and treatment of chemicals.

Structure	Name	Source	Treatment
CH_3OH	Methanol	American Scientific	Distillation
CH_3CH_2OH	Ethanol	Commercial Solvents Corporation	Distillation
$CH_3CH_2OCH_2CH_3$	Diethyl ether	Mallinkrodt	Distillation
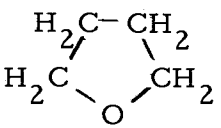	Tetrahydrofuran	Baker Analyzed Reagent	Distillation
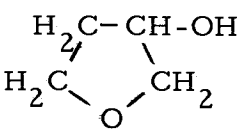	3-Hydroxytetrahydrofuran	Aldrich	GLC (prep)[1]
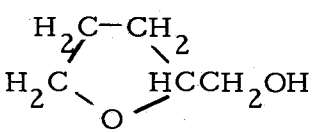	Tetrahydrofurfuryl alcohol	Aldrich	GLC (prep)
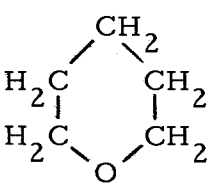	Tetrahydropyran	Aldrich	GLC (prep)
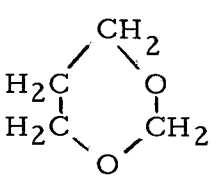	1, 3-Dioxane	Pfaltz and Baur	Distillation and GLC (anal)[2]

Table 1. Continued.

Structure	Name	Source	Treatment
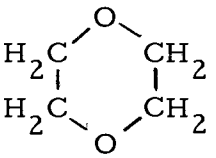	1, 4-Dioxane	Baker Analyzed Reagent	GLC (anal)
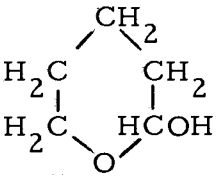	2-Hydroxytetrahydropyran	Synthesized by Author	GLC (prep) n^{24} = 1.4523 (measured) n_D^{25} = 1.4513 (49)
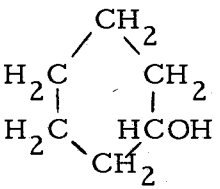	Cyclohexanol	Baker Analyzed Reagent	GLC (prep) n^{22} = 1.4657 (measured) n_D^{22} = 1.4650 (3)
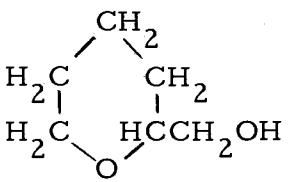	Tetrahydropyran-2-methanol	Aldrich	GLC (prep)
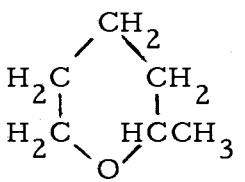	2-Methyltetrahydropyran	Aldrich	GLC (prep)

[1]Gas-liquid chromatography preparative, Column described in text.
[2]Gas-liquid chromatography analytical, Column described in text.

When the collection was complete, 2 to 3 μl were reinjected to show that the sample had been purified.

The 1, 3-dioxane was technical grade, so it was treated to remove peroxides. The sample was refluxed for 5 hours in the presence of solid sodium. Then it was fractionally distilled with only the middle 20% being saved. The spectrum of this material was indistinguishible from untreated 1, 3-dioxane.

The four low boiling compounds, methanol, ethanol, diethyl ether and tetrahydrofuran were of excellent grade, but could not be chromatographed practically since they came off the column too soon. Spectra of all of these were available (5, 10, 11, 32) which agreed very well with my spectra of untreated samples. Fractional distillation was performed on all of these with only the middle 20% being saved. This treatment had no effect on the spectra.

An independent measure of compound purity was obtained from the refractive index. The data for simple compounds is readily available (3). We used the Abbé-3L Refractometer by Bausch and Lomb to indicate the composition of the samples.

The 2-hydroxytetrahydropyran was synthesized by acid hydration of dihydropyran following the method of Woods (49, vol. 3, pages 470-471). Since the refractive index of my product was 1.4523 at 24° C as compared to n_D^{25} 1.4513 for the reported value, the only purification performed was the GLC distillation described previously.

Measurement of the Spectra

The samples which had been purified as described in the previous section were all outgassed immediately after purification. This was done by freezing and thawing them under a vacuum. This was repeated at least three times. When the MKS Baratron gauge was obtained, it was possible to measure the rate of dissolved gas leaving the sample, so one could merely pump on the sample until the gas was gone.

In measuring the spectra, the first step was to record a baseline with the cell under vacuum. The scan speed in initial spectra was 100 to 200 Å per minute with the chart speed set at 2 inches per minute. Next a little sample was let into the system and brought to equilibrium. Several spectra of the sample were taken at constant room temperature, but different pressures. The material was pumped away and replenished between spectra. When the absorbance versus pressure ratios were compared at constant wavelength and temperature some information could be obtained about photodecomposition and sample purity. When the ratios, which are directly proportional to the extinction coefficients, remained constant over several spectra, they were considered reliable. No evidence of photodecomposition was observed. When the compound's spectrum had been published, it was compared to my own results.

The method of measuring the pressure was determined by the vapor pressure of the sample at room temperature. Highly volatile compounds were measured directly on the U tube mercury manometer if the 1 mm path length cell was used. The pressure could also be measured indirectly with a bulb expansion technique and a 100 mm cell. This involved introducing a large measured amount of vapor into the system and trapping a known volume of it in a glass bulb. After the rest of the system had been evacuated and sealed, the material in the sphere was released into a larger known volume including the cell and its spectrum recorded. For less volatile compounds, the 10 mm and 100 mm cells were used with the oil gauge or the MKS Baratron gauge. The latter is the most versatile and easiest to use. Extinction coefficients for ethanol obtained by the four different techniques are given in Table 2.

Table 2. Extinction coefficients of ethanol measured by four different methods at 1525 Å.

Method	Extinction Coefficient
Capacitance manometer	4001
U tube mercury manometer (direct)	4130
U tube mercury manometer (expansion)	3950
Micrometric manometer (dibutyl phthalate)	3980
Difference between highest and lowest = 180	
180/4000 $\cong$ 4.5% variation.	

The final spectra were taken at a scan speed of 20 Å per minute with the chart speed 2 inches per minute, to spread the spectrum. The study of each compound was carried out at least twice several months apart. If any changes were noted, further work was done.

Spectra

Introduction

The spectra can be divided into three classes: 1, simple alcohols; 2, simple ethers; and 3, cyclic ether - alcohols and dioxanes. The shape of the spectra seem to be more closely related to the structure of the oxygen group, i.e., whether it is an ether or an alcohol, than to the hydrocarbon skeleton. These similarities led us to believe that a simple theory for the electronic structure of sugars could be developed.

In this section the spectra are presented and discussed briefly. Most of the interest in this section is directed at the region in energies below 70 kK. Later in the theoretical section an argument will be developed that these bands are due to transitions of the nonbonding oxygen electrons. Finally it will be shown that by combining these transition bands for some of the simple alcohols and ethers, one can arrive at a fairly accurate prediction of the spectra for some of the complex compounds.

Simple Alcohols

This set consists of methanol, ethanol and cyclohexanol which are shown in Figures 2, 3 and 4. The first two were recorded earlier (5, 10) but were repeated on our instrument so that their measured extinction coefficients would be comparable to the other compounds. All these show a broad, low band between 50 and 60 kK. Both methanol and ethanol have more distinct peaks in the 60 to 70 kK region with much higher extinction coefficients. Edwards (5) calls the two peaks at 67 and 68 kK in methanol and the two at 65 and 66 kK in ethanol Rydberg 2p transitions. Unpublished spectra of 2-butanol (46) and isopropanol (18) also show transitions at 64 kK. In the cyclohexanol, only a shoulder appears in this region. This molecule was included because it is a cyclic alcohol, as are all the alcohol groups in the alcohol-ether set and in the sugars themselves.

Simple Ethers

There are four simple ethers, diethyl ether, tetrahydrofuran, tetrahydropyran and 2-methyltetrahydropyran shown in Figures 5 through 8. Spectra of diethyl ether (5, 11, 13), tetrahydrofuran (14, 32) and tetrahydropyran (14, 32) have been reported previously.

In studying these ethers, one should note that the first two, diethyl ether and tetrahydrofuran, are very much alike. Both have

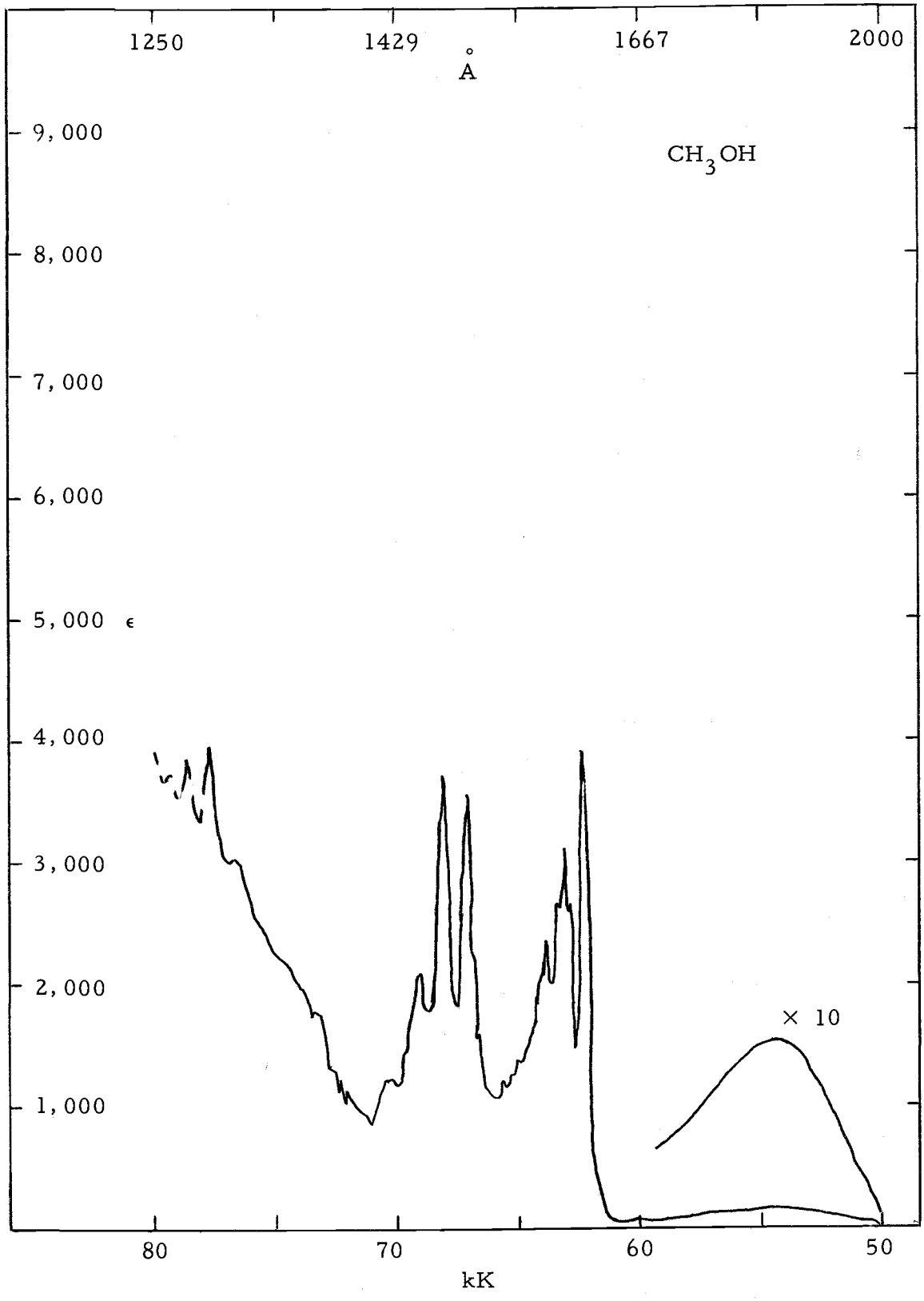

Figure 2. Methanol.

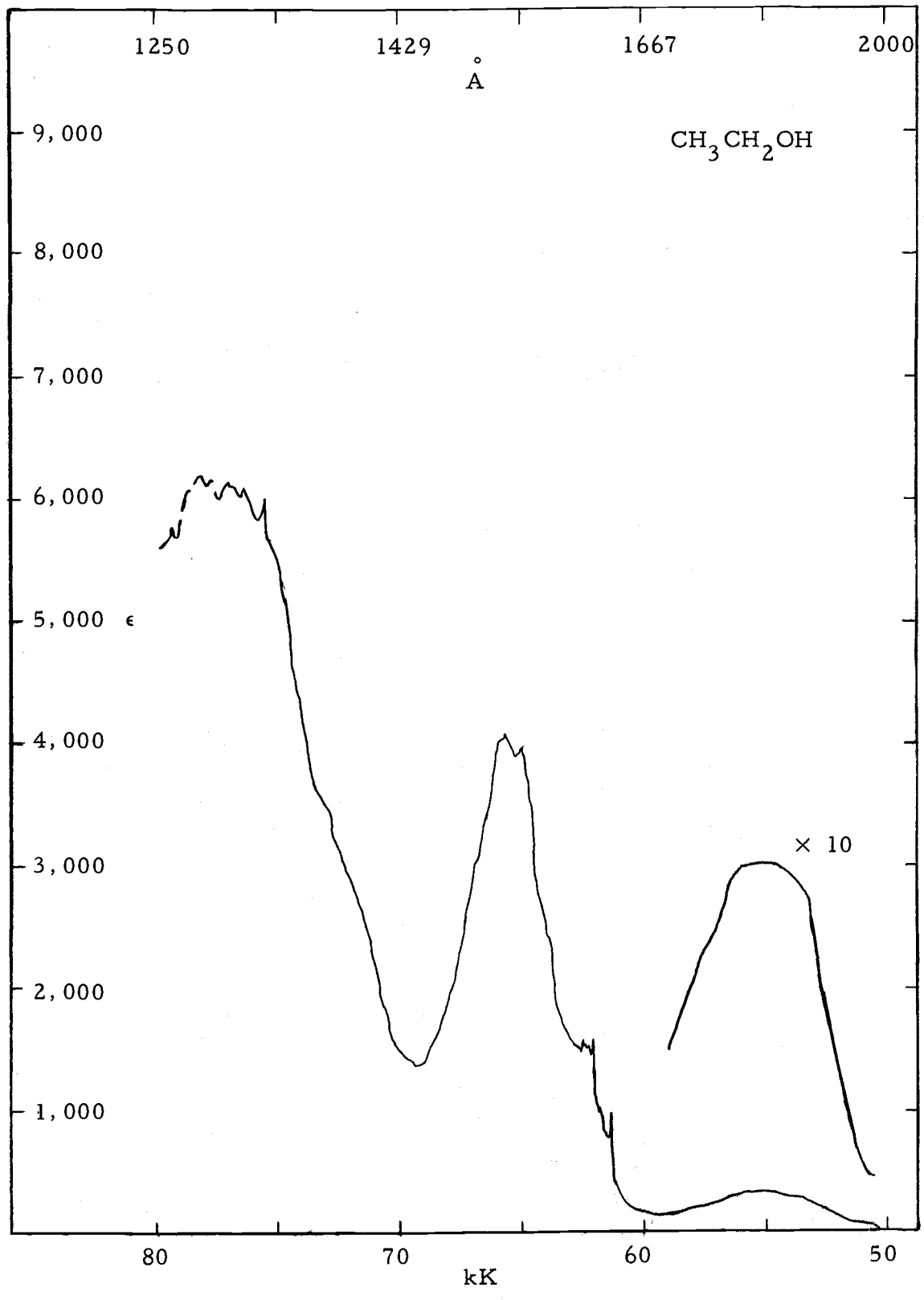

Figure 3. Ethanol.

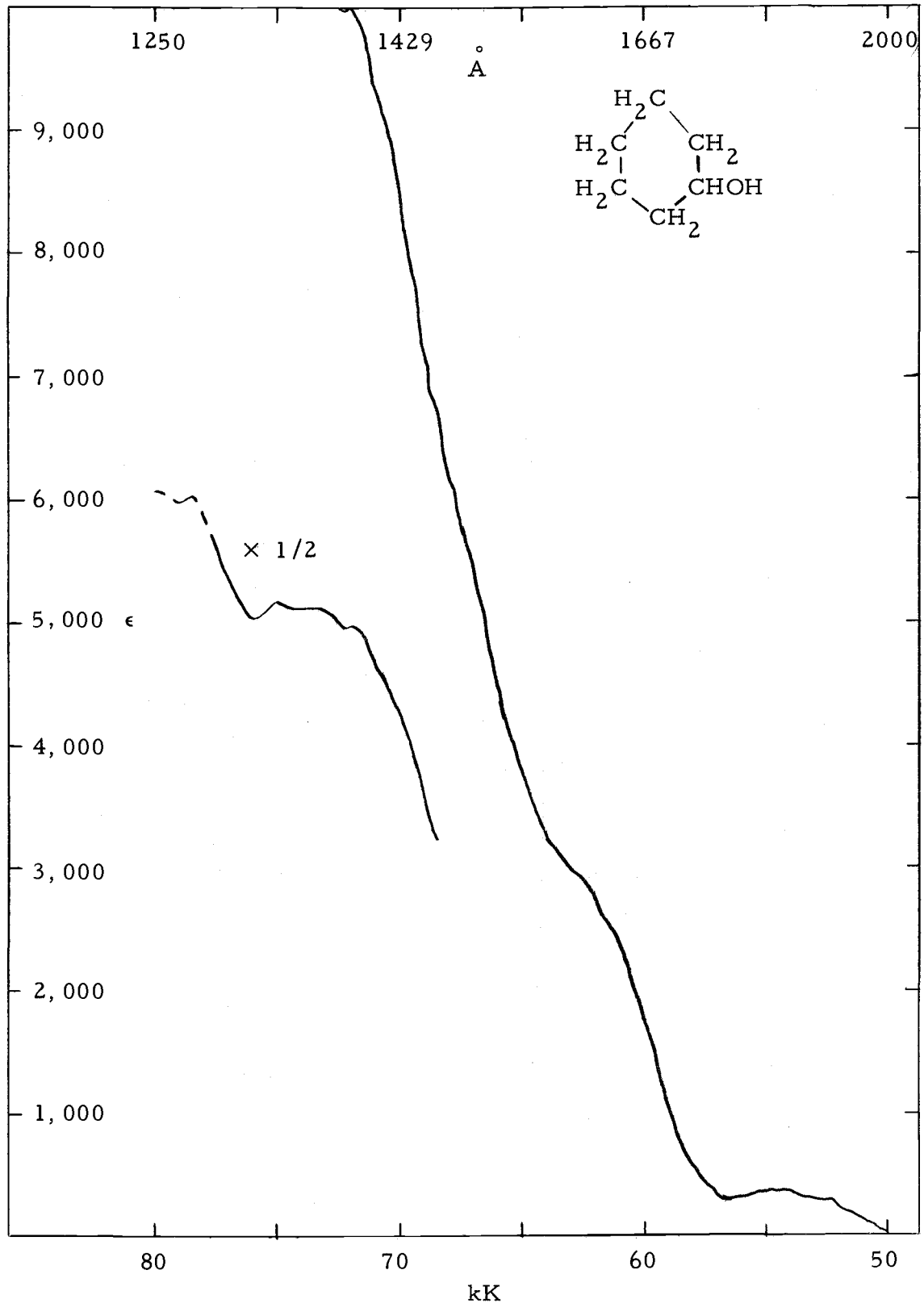

Figure 4. Cyclohexanol.

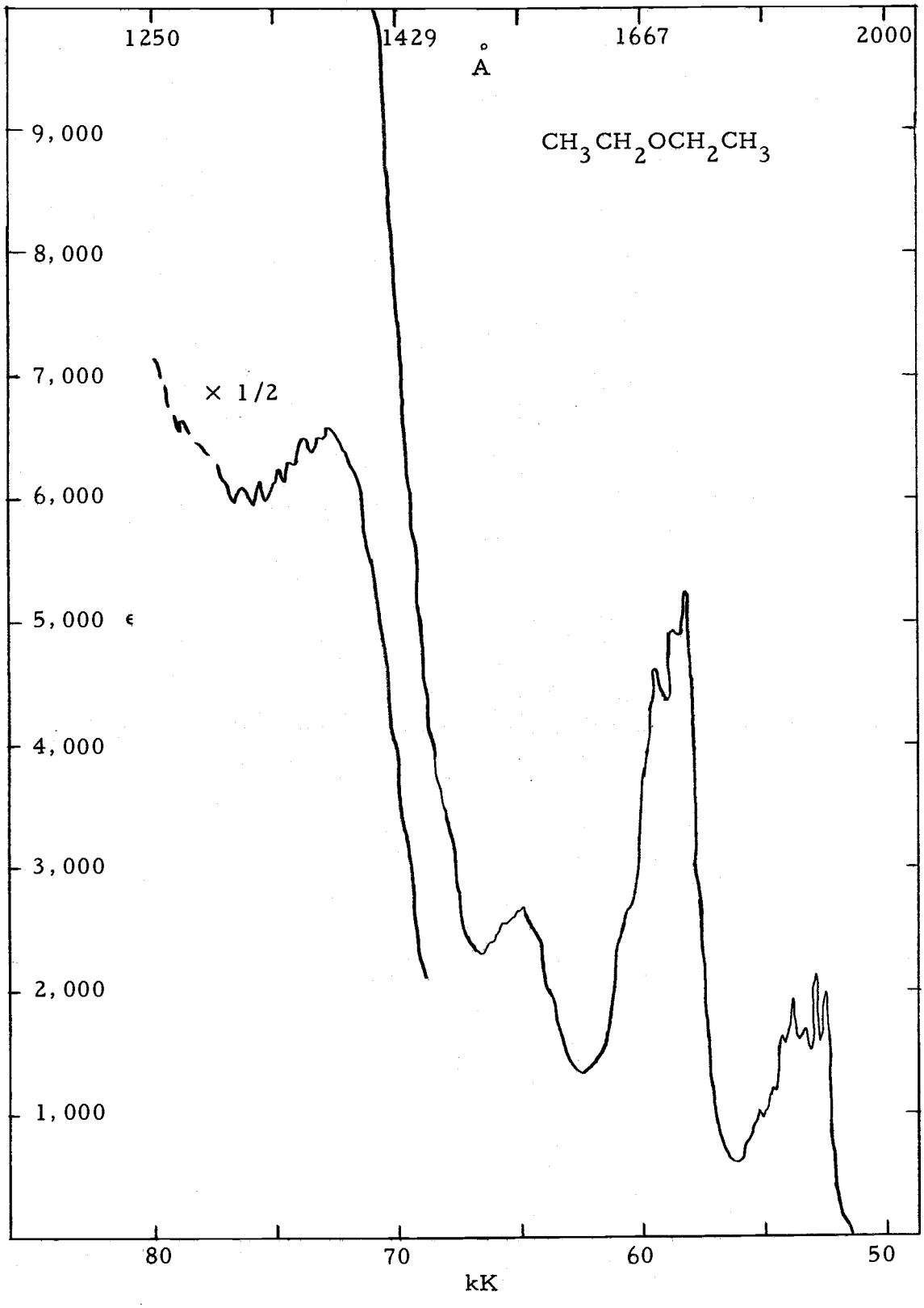

Figure 5. Diethyl ether.

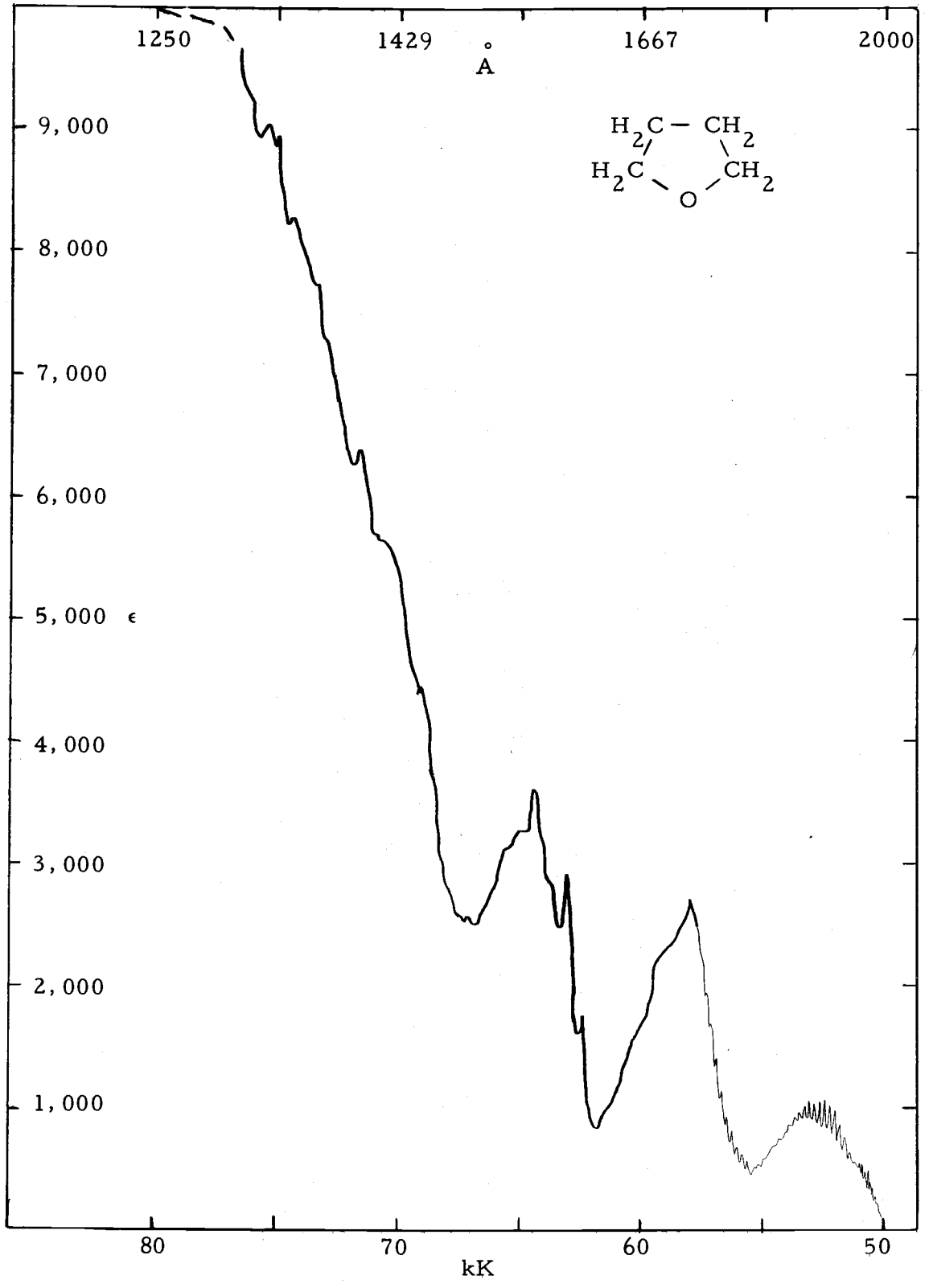

Figure 6. Tetrahydrofuran.

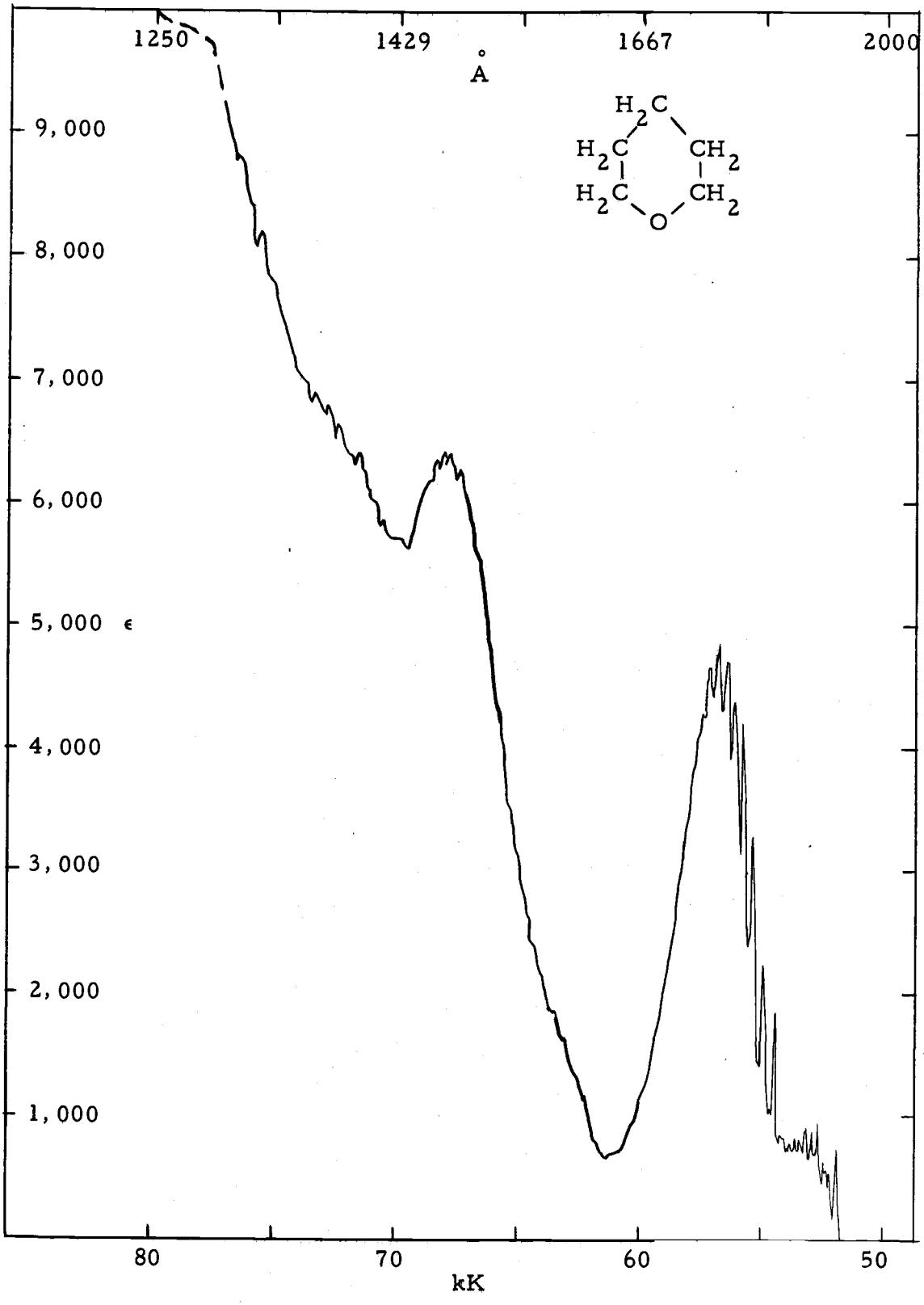

Figure 7. Tetrahydropyran.

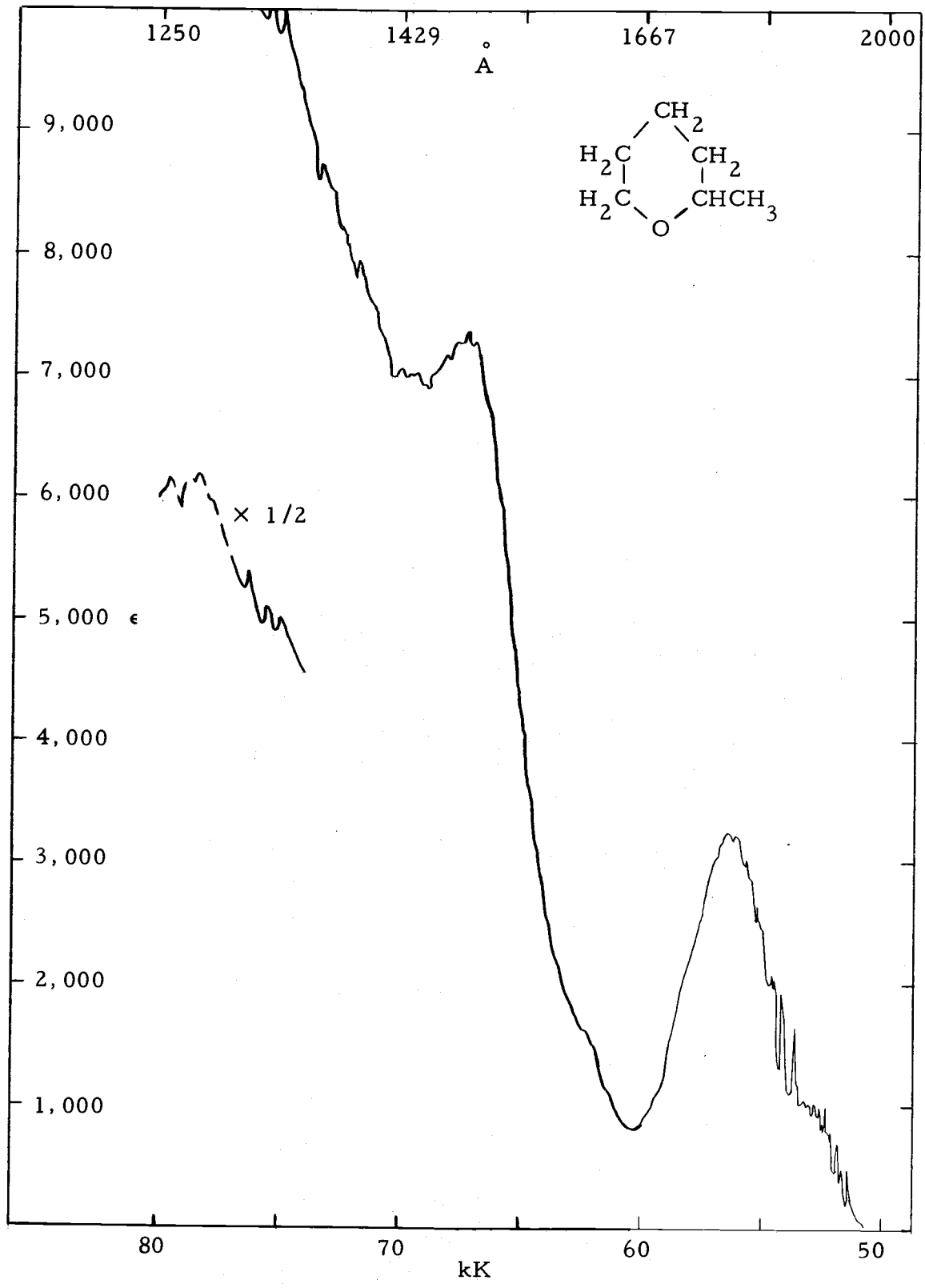

Figure 8. 2-Methyltetrahydropyran.

three major peaks in the spectral region 50 to 67.5 kK. These are centered at almost the same energies: 53 kK, 58 to 59 kK and 64 to 65 kK. These peaks show fine structure and have been studied by Hernadez for an assignment of the vibronic structure. Both of the molecules have the same types of bonds. The only difference between them is that tetrahydrofuran is cyclic and thus has one more CC bond and two fewer CH bonds.

The two six-membered ring compounds, tetrahydropyran and 2-methyltetrahydropyran, are also strikingly similar. Both have highly structured but low peaks at 50 to 55 kK which are partially hidden by higher peaks centered at 56 to 57 kK. In the 2-methyl-tetrahydropyran the 56 kK peak is lower and much less structured. Considering the similarities between the compounds' structures, the spectral resemblances should not be surprising at this point.

Cyclic Ether-Alcohols and Dioxanes

The set of cyclic ether-alcohols consists of 3-hydroxytetrahydrofuran, tetrahydrofurfuryl alcohol, 2-hydroxytetrahydropyran and tetrahydropyran-2-methanol. These appear in Figures 9, 10, 11 and 12. All these compounds are closely related to sugar monomers. These spectra are all new. None of these spectra exhibit any fine structure. The first two are both five membered rings with an OH group attached to the ring in the 3 position in the first case and a CH_2OH group

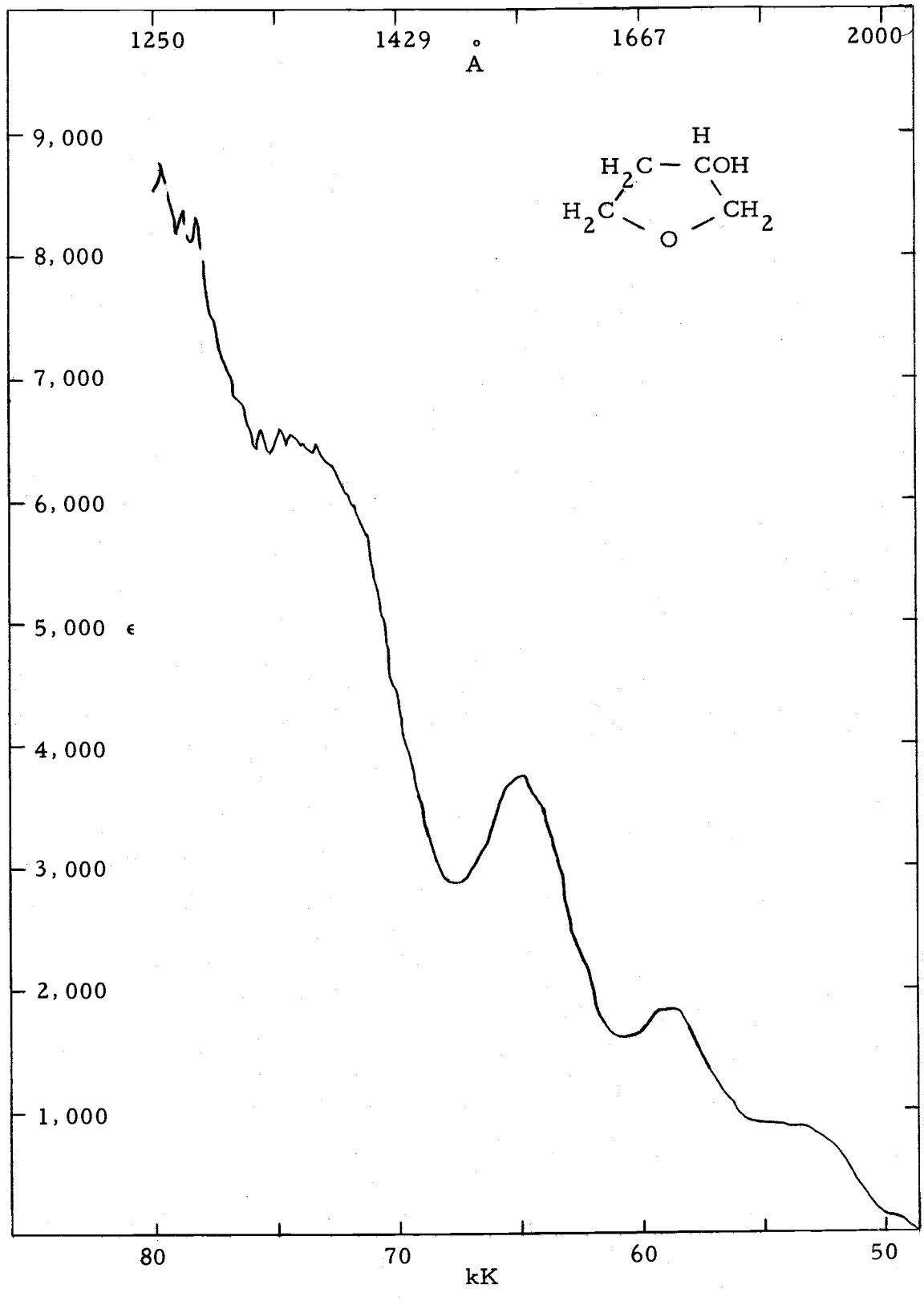

Figure 9. 3-Hydroxytetrahydrofuran.

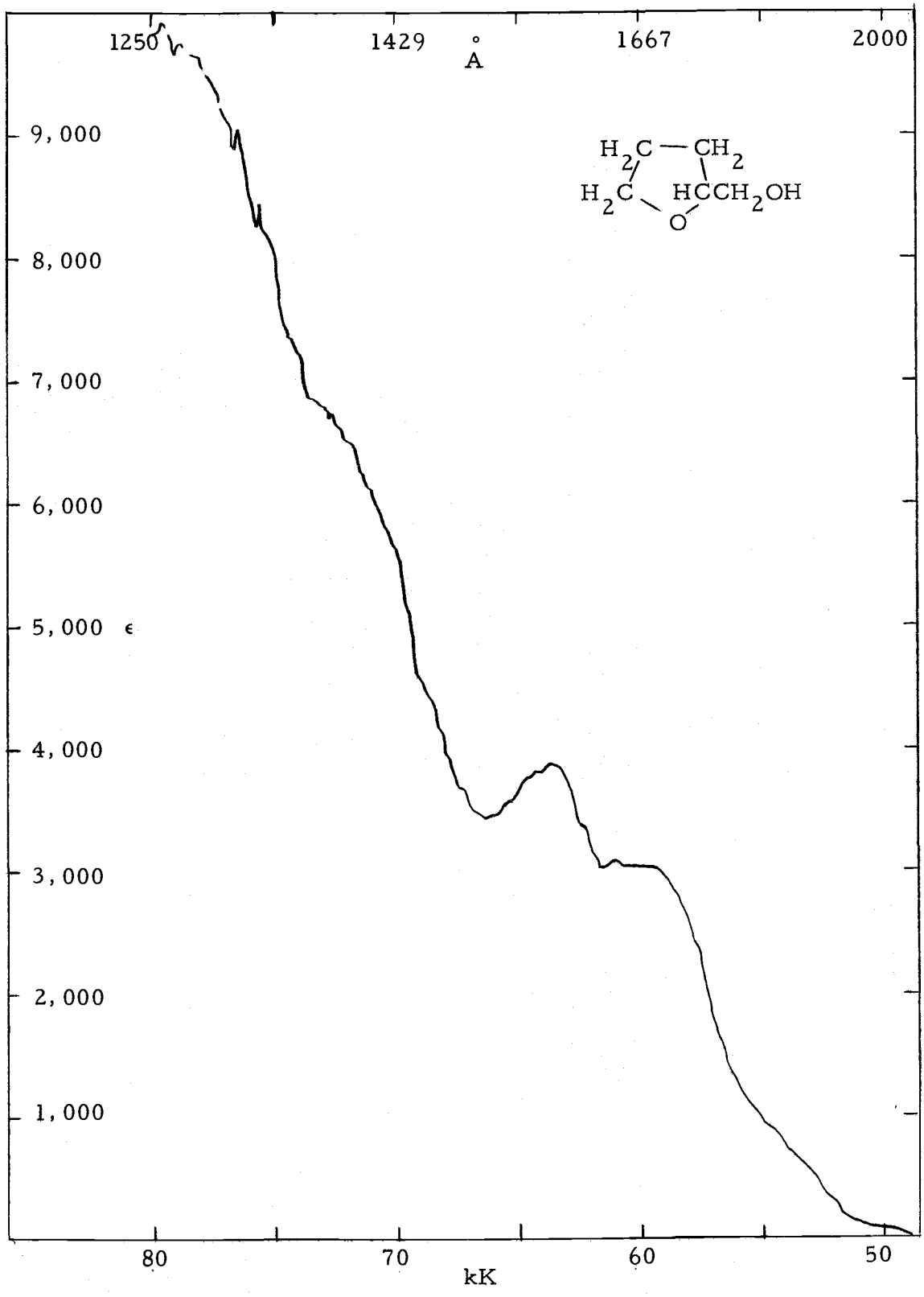

Figure 10. Tetrahydrofurfuryl alcohol.

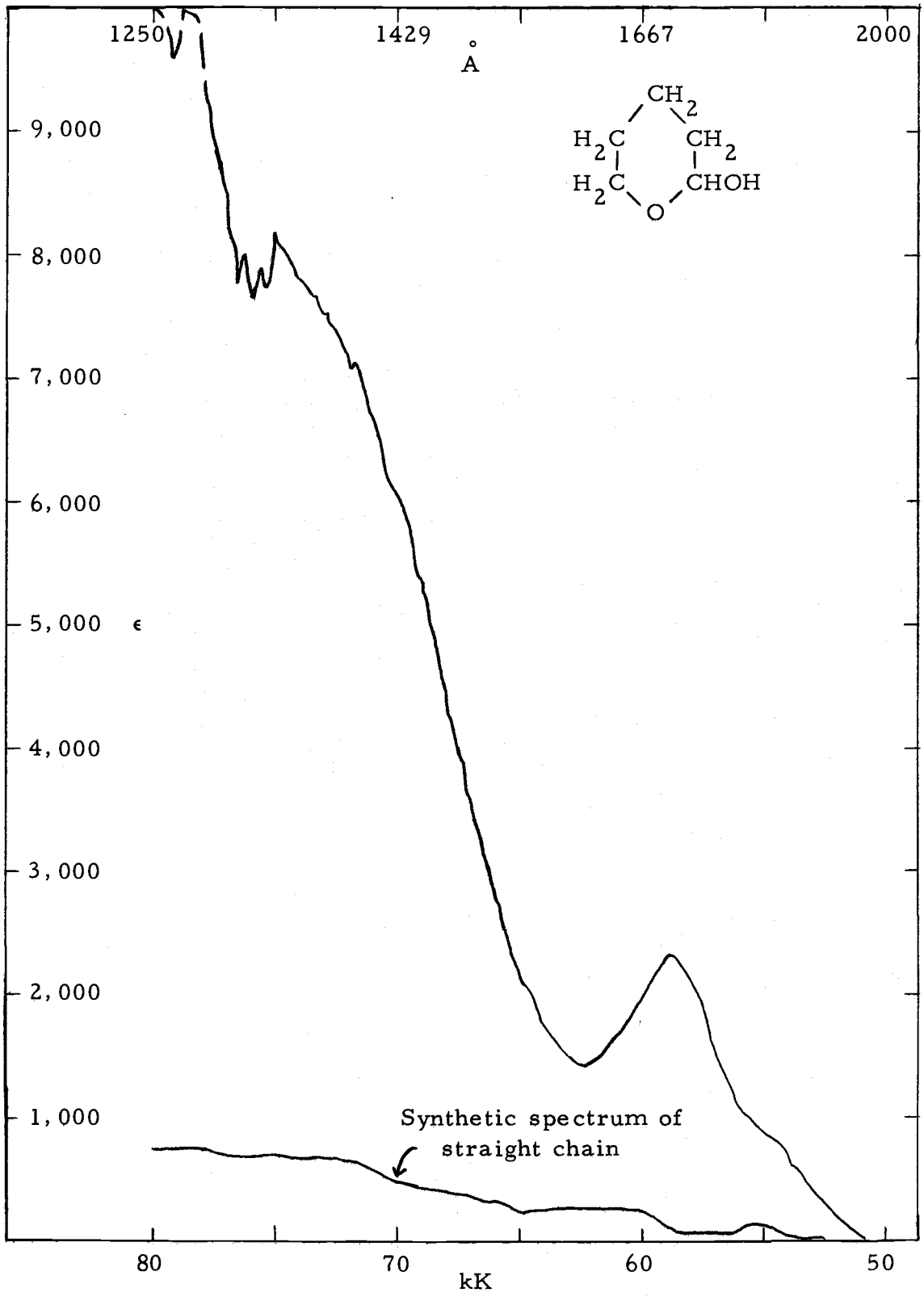

Figure 11. 2-Hydroxytetrahydropyran.

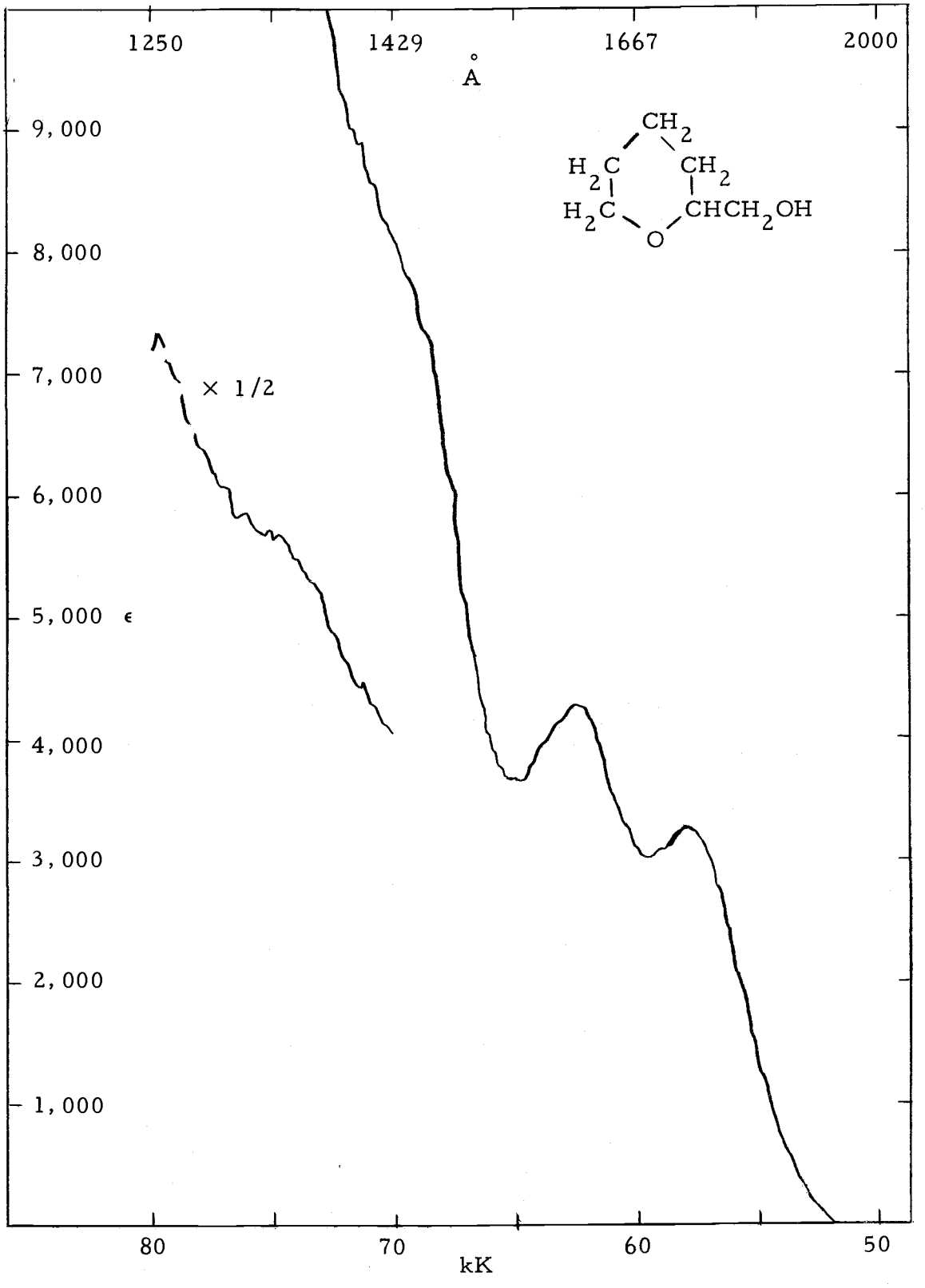

Figure 12. Tetrahydropyran-2-methanol.

attached to the ring in the 2 position in the second. The spectra are fairly similar, with the 65 kK peak in 3-hydroxytetrahydrofuran shifted to 63.5 kK in the tetrahydrofurfuryl alcohol. Both have peaks at 58 to 59 kK, but the distinct shoulder at 54 kK in the first compound appears to have been blue shifted so much that only a hint of it is seen in the second compound.

The fourth compound, tetrahydropyran-2-methanol, is different from tetrahydrofurfuryl alcohol only in ring size, since they both have CH_2OH groups attached to the ring at the 2 position. For spectral differences, the two peaks in the six membered ring are red shifted about 1 kK and the shoulder at 55 kK has disappeared.

The 2-hydroxytetrahydropyran differs from all the others in that the ring can open or close.

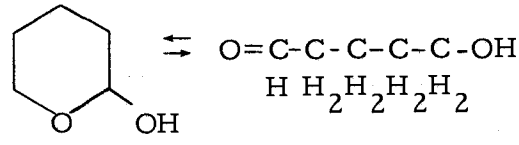

This is similar to the situation of monosaccharides. In order to interpret the lower energy part of the spectrum we must know whether the majority of the molecules in the vapor phase are cyclic or straight chain. The bonds attached to the oxygen atoms are quite different in the cyclic case than in the straight chain.

We cannot obtain spectral evidence to support either form in the vapor phase, since under the prevailing conditions of temperature and

pressure even a 100% vapor solution of the straight chain form would not have shown a detectable $n-\pi^*$ transition for the C=O bond. This is because the extinction coefficient for this transition is very low. In an attempt to estimate the amount of straight chain in the vapor, we measured the absorbance spectrum of a .0054 Molar solution of 2-hydroxytetrahydropyran in cyclohexane. The composition in this solution should be similar to that in the vapor phase. Under this condition, the compound shows an extinction coefficient at 2900 Å of 0.45. The minimum extinction coefficient of the pure straight chain $n-\pi^*$ transition is about 10, so this corresponds to at worst 4.5% straight chain and 95.5% ring form. Approximately the same percentages are found in aqueous solution (42).

It is fairly certain that the straight chain form has absorption bands for both the alcohol and the aldehyde group in the region 50 to 65 kK. Later in this work we show that the spectrum in this region of this type of compound should be approximately the sum of the bands of the two oxygen groups. We have no spectra available of pentanal or of 1-pentanol. However, we do have spectra of 2-butanol (46) and of propionaldehyde (2), which we believe would be fairly similar to the longer chain compounds. We have plotted below the spectrum of the 2-hydroxytetrahydropyran a new spectrum which is 5% as high as a sum of propionaldehyde and 2-butanol. There are sharp peaks in the actual propionaldehyde which have been smoothed here since they are

not present in the spectrum of 2-hydroxytetrahydropyran.

The 59 kK peak for this compound could perhaps be related to the 57 kK peak for tetrahydropyran in Figure 7.

The two dioxanes are shown in Figures 13 and 14. The 1,4-dioxane (15,32) is very similar to tetrahydropyran in the energy region below 70 kK. The 56 to 57 kK peak seems in fact to have doubled in intensity for 1,4-dioxane corresponding to a doubling of the number of oxygen atoms in the ring. The peaks are very structured in both 1,4-dioxane and tetrahydropyran. The 1,3-dioxane (15) looks somewhat like the 1,4-dioxane, but is blue shifted by 8 kK. The structural difference is that the 1,3-dioxane has an OCO group in the ring, while in 1,4-dioxane the oxygen atoms are separated by 2 carbon atoms. The same OCO group would exist in the 2-hydroxytetrahydropyran and in sugars. It may be that the nonbonding electrons on the two oxygens are close enough together to interact in these two cases.

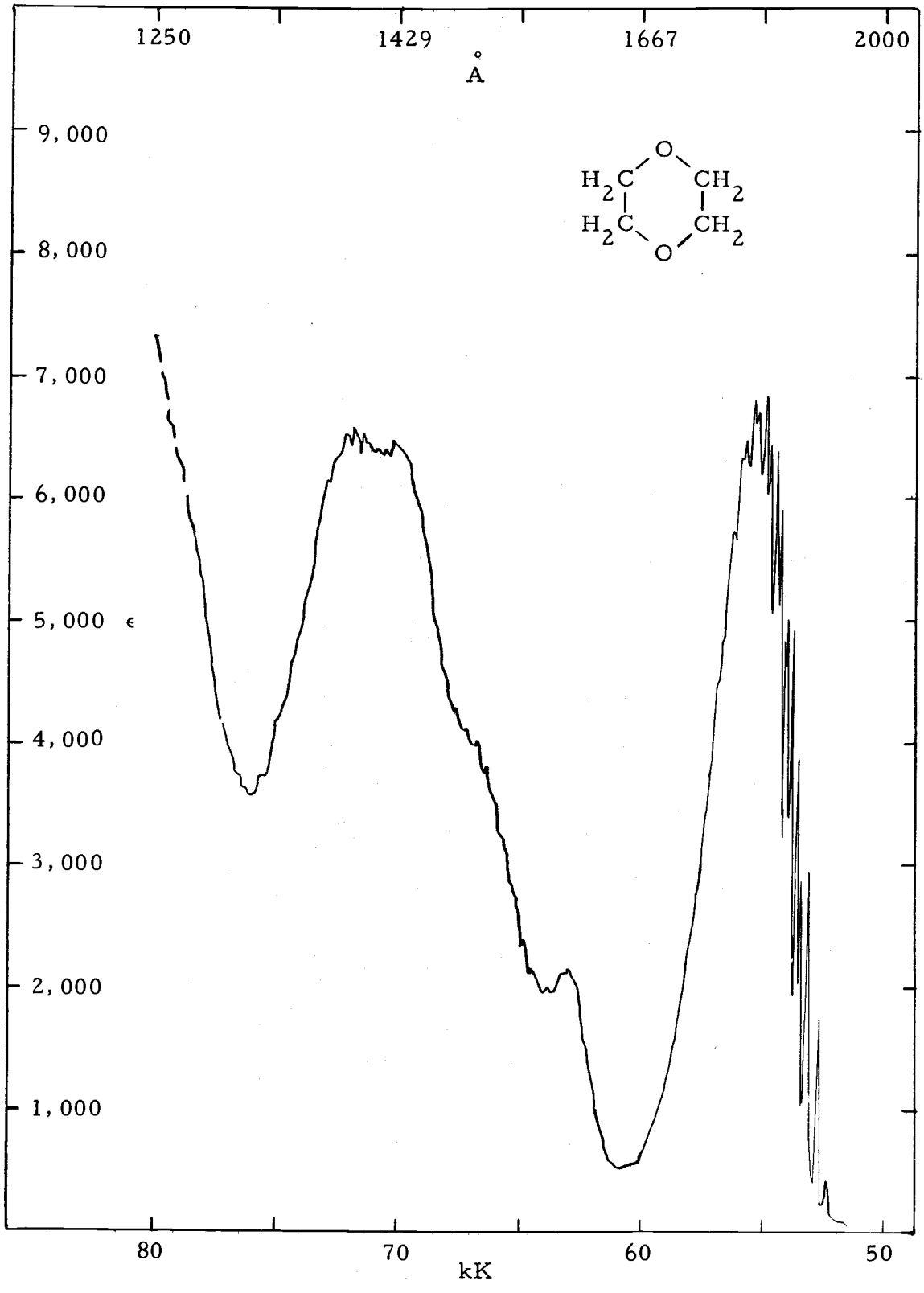

Figure 13. 1,4-Dioxane.

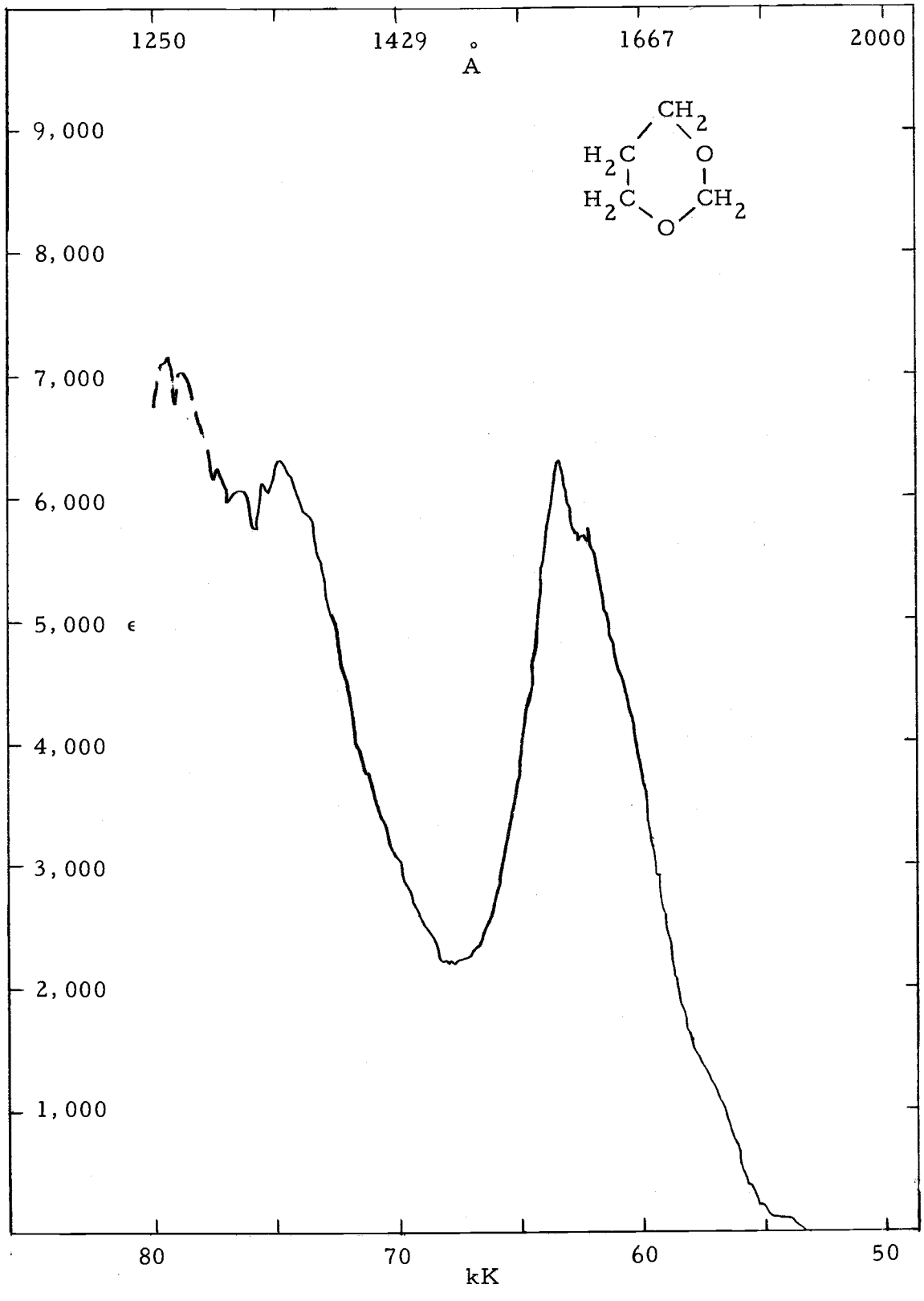

Figure 14. 1,3-Dioxane.

THEORETICAL CALCULATIONS OF $\sigma \rightarrow \sigma^*$ BANDS FOR MODEL SUGAR COMPOUNDS

Introduction

The goal of this calculation is to prove that in the model sugar compounds, the spectral bands which lie below 67 kK arise from transitions of the 2p nonbonding electrons on oxygen. This information is necessary to interpret the circular dichroism studies on simple sugars and oligosacchardies which are currently being carried out by this group (27). Simple monosaccharides contain the same types of bonds as do the model compounds. They differ only in that they have a greater number of hydroxyl groups. For instance, 2-deoxyribose has only two more hydroxyl groups than tetrahydrofurfuryl alcohol or 3-hydroxytetrahydrofuran. Thus, the nonbonding electronic transitions of 2-deoxyribose are related to those of 3-hydroxytetrahydrofuran and tetrahydrofurfuryl alcohol.

In the present work we first show that the low energy transition bands are related to the presence of the oxygen atoms in the model sugar compounds. This is easily done by comparing the spectrum of any of these compounds to that of the corresponding hydrocarbon.

Next, we prove that these bands are due to excitations of the oxygen nonbonding electrons. We cannot do this directly. All oxygen atoms in model sugar compounds have eight outer shell electrons.

Four of these are in two different nonbonding orbitals which include one low energy orbital that is mainly 2s and another high energy orbital that is mainly 2p (7). The other four electrons are in two bonding orbitals. In alcohol, for example, there are two different bonding orbitals on the oxygen, one forming the CO bond and the other forming the HO bond. Thus, we cannot simply measure an oxygen nonbonding transition spectrum, since even the simplest oxygen containing molecules, such as water or methanol, have intravalence shell transitions.

Thus, we want to calculate the spectrum of the $\sigma - \sigma^*$ transition for the model sugar compounds. From this we can see if any transition bands are predicted below those of the hydrocarbons in the energy region of 50 to 65 kK.

Our method for obtaining the theoretical spectra is the independent systems approach as described by Simpson (45). In the following sections we describe the independent systems method. This method requires a knowledge of the transition energies of the appropriate isolated bonds as well as their energies of interaction with other bonds in the molecule. Subsequently we describe how these energy values were obtained. Then we perform the calculations of the $\sigma - \sigma^*$ spectra from the independent systems method.

The $\sigma - \sigma^*$ transition energies calculated for some hydrocarbons and model sugars are compared with the experimental transition

energies for the model sugars. Since low energy transitions are, indeed, missing from the calculated results, it is concluded that the low energy transitions are from nonbonding electrons of the oxygen.

Finally, an attempt is made to show that the low energy transitions of the simple molecules can be combined graphically to give predicted spectra of the more complex examples.

Comparison of Model Sugar Compounds With Related Hydrocarbons

We wish to establish a relationship between the oxygen atoms in the model sugar compounds and the low energy bands in their absorption spectra. Thus we compare these spectra of simple alcohols and ethers to those of corresponding hydrocarbons (38). We first compare methanol and ethanol to ethane and propane. We are replacing the hydroxyl group on the alcohols by a methyl group in this argument. As can be seen in Figure 15, the ethane has a small peak at 70.5 kK, but nothing at lower energies. The methanol, however, has several peaks in the region 50 to 70 kK.

Similarly, the spectrum of propane begins to rise at 62.5 kK. The first broad, low intensity band is a charge transfer transition (38, page 62). Its peak is hidden by higher energy transitions. This charge transfer band has no sharp peaks like the ethanol does at 65 kK. There may be CO charge transfer bands underlying the

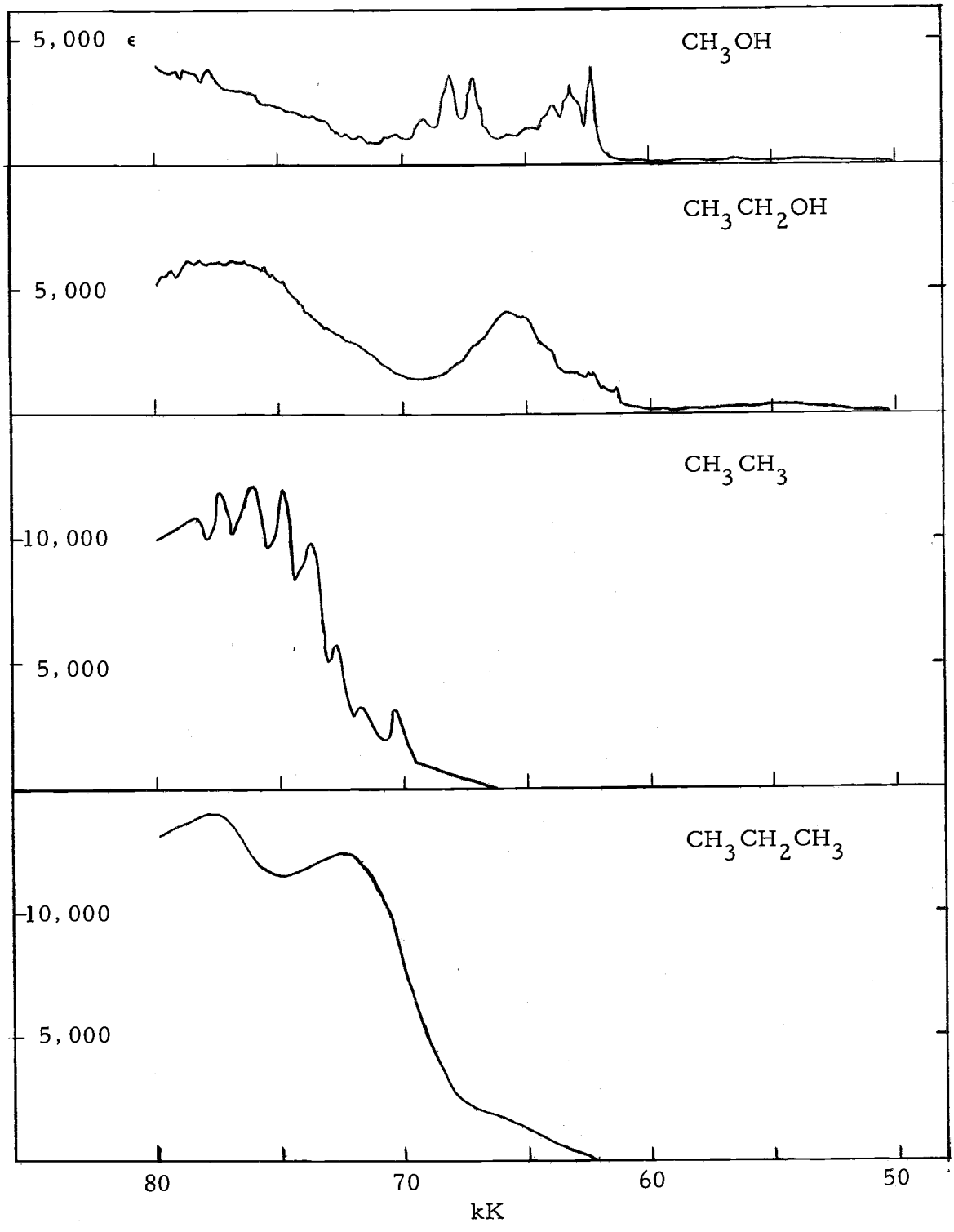

Figure 15. Comparison of alcohols to hydrocarbons.

nonbonding transitions in the model sugar compounds. These bands come at higher energies in the hydrocarbons than the 50 to 65 kK series of bands which the ethanol exhibits.

Turning to Figure 16, we note that pentane has a continuously rising spectrum from 61.5 kK on to higher energies. The two ethers, however, have peaks at 53, 58 and 65 kK. The spectrum of cyclopentane differs only slightly from linear pentane, and the conclusion is the same whichever is used for the comparison.

Thus, we can at least state that the low energy peaks in the model sugars are related to the oxygen atoms in the molecules. However, as pointed out in the introduction to this section, we cannot tell whether they are related to the CO, or OH bonding electrons or to the 2p nonbonding electrons on the oxygen.

Independent Systems Approach to Model Sugar Spectra

The Model

We will treat the molecule as a set of bonds, each of which consists of two valence electrons located between two positively charged centers. We ignore electron exchange between bonds. Each type of bond is assumed to have a fundamental electronic transition energy, and each pair of neighboring bonds has a characteristic interaction energy, regardless of their positions within the molecule.

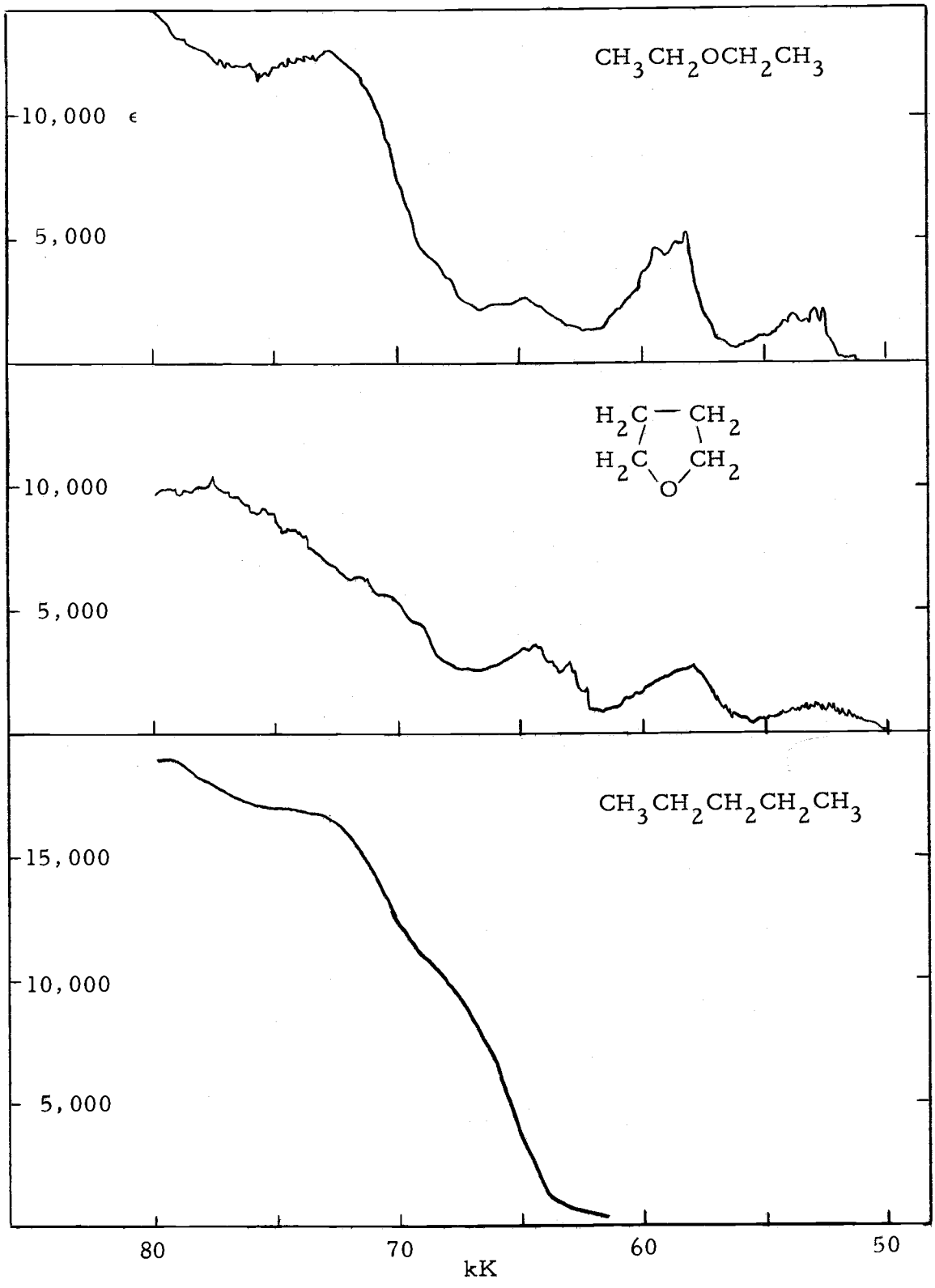

Figure 16. Comparison of ethers to hydrocarbon .

The Independent Systems Theory

This approach has been studied in detail (23, 45) and used by several workers (40, 43, 44). In particular, Raymonda has used this method in the prediction of the spectra of alkanes (37, 38). His results are quite consistent with experiment. The only changes from his system to ours are in the method of arriving at the localized bond transition energies and in the fact that we have added CO and OH bonds to the system. His success gives us confidence that our results should be reliable.

We shall now outline the basic apparatus needed for carrying out this calculation. Let us begin by defining the Hamiltonian which describes a system of N bonds. With no interaction between bonds,

$$H = \sum_{i}^{N} h_i \tag{3}$$

Where h_i is a local Hamiltonian for a bond i shown in Figure 19.

$$h_i = -\frac{\hbar^2}{2m_e}(\nabla^2(1)+\nabla^2(2)) - \frac{e^2}{r_{1A}} - \frac{e^2}{r_{1B}} - \frac{e^2}{r_{2A}} - \frac{e^2}{r_{2B}} + \frac{e^2}{r_{12}} \tag{4}$$

where A and B represent the two centers, and 1 and 2 the two electrons. The factor m_e is the mass of an electron and $\hbar$ is Plank's constant divided by 2π. When interaction between bonds

is introduced,

$$H' = \sum_{i}^{N} h_i + \frac{1}{2} \sum_{i \neq j}^{N} V_{ij} \,. \tag{5}$$

The term V_{ij} is the electrostatic interaction potential between the two bonds i and j. In order to find energies for these Hamiltonians, we must have molecular wave functions.

For the ground state of the unperturbed system

$$\Phi^0 = \prod_{i}^{N} \phi_i^0 \tag{6}$$

where each ϕ_i^0 is a normalized wave function for a particular localized bond i. The Φ^0 terms will not be antisymmetrized since we are ignoring electron exchange between bonds. The ϕ_i^0 each contain two electrons of opposite spin. Each ϕ_i^0 must satisfy the Hamiltonian for the bond

$$h_i \phi_i^0 = E_i^0 \phi_i^0 \tag{7}$$

There is a set of N different wave functions for singly excited states.

$$\Phi^i = \phi_i^+ \prod_{j \neq i}^{N} \phi_j^0 \tag{8}$$

Here one of the electrons in one of the bonds in the molecule is

excited while the rest are still in the ground state. We neglect multiply excited states.

Again, the Hamiltonian for each bond must be satisfied.

$$h_i \phi_i^+ = E_i^+ \phi_i^+ \tag{9}$$

This excited state energy lies above the ground state unperturbed energy by the amount

$$E_i^+ - E_i^0 \equiv a_i . \tag{10}$$

In the present work, these quantities a_i are to be estimated by the extended Huckel method and also by the CNDO approximation. These methods will be discussed in detail in the next two sections.

The wave functions for the perturbed system are approximated as linear combinations of the functions described in formulas (6) and (8)

$$\Psi^K = \sum_{i=0}^{N} c_{iK} \Phi^i \tag{11}$$

These functions belong to the eigenvalue λ_K of the secular equation. The functions include the ground state and all singly excited states. Since for the ground state the energy $a_0 = 0$, the coefficient c_{0K} is also zero. Thus, the secular equation will have only N nonzero solutions.

The squared coefficient $|c_{iK}|^2$ gives the probability that bond i is excited when the molecule is in excited state K. The sign of c_{iK}

gives the relative phase of the excitation in bond i. If c_{iK} is less than zero the relative phase is opposite from that chosen in the reference state. The phase may be represented by arrows along the bond, as shown in the following example.

The variation method, which is described in the next section, is used to determine the c_{iK}'s and the eigenvalues λ_K. The off-diagonal elements which occur in the secular equation of the variation method are the electrostatic interaction potentials V_{ij}.

$$(\Phi^k|\frac{1}{2}\sum_{i\neq j}^{N} V_{ij}|\Phi^\ell) = (\phi_k^+\phi_\ell^0 \prod_{r\neq k,\ell} \phi_r^0|\frac{1}{2}\sum_{i\neq j}^{N} V_{ij}|\phi_k^0\phi_\ell^+ \prod_{s\neq k,\ell} \phi_s^0)$$

$$= (\phi_k^+\phi_\ell^0|V_{k\ell}|\phi_k^0\phi_\ell^+)(\prod_{r\neq k,\ell} \phi_r^0|\prod_{s\neq r,\ell} \phi_s^0)$$

$$= (\phi_k^+\phi_\ell^0|V_{k\ell}|\phi_k^0\phi_\ell^+) \equiv \beta_{k\ell} \qquad (12)$$

Thus, $\beta_{k\ell}$ is the intramolecular interaction energy for the system.

Example

We now wish to illustrate this method with a simple example. Let us consider water. The reference basis state is taken as in Figure 17. The transition is considered to be along the bond in the directions of the arrows.

The secular equation associated with this system is simply:

$$\begin{vmatrix} \alpha_1-\lambda & \beta_{12} \\ \beta_{12} & \alpha_2-\lambda \end{vmatrix} = 0 \qquad (13)$$

Where the subscripts refer to the two different OH bonds. This has the following solutions and corresponding wave functions:

$$\Psi^{+} = \frac{1}{\sqrt{2}} (\Phi^{1} + \Phi^{2}) \qquad \lambda = \alpha + \beta_{12}$$
$$\Psi^{-} = \frac{1}{\sqrt{2}} (\Phi^{1} - \Phi^{2}) \qquad \lambda = \alpha - \beta_{12} \tag{14}$$

Since $\alpha_1 = \alpha_2$. This splitting pattern is depicted in Figure 18. Note that in Ψ_-, the phase of the excited state in bond 2 is opposite to that chosen in the reference state. Thus the arrows are shown as head-to-tail in the Ψ_- excitation.

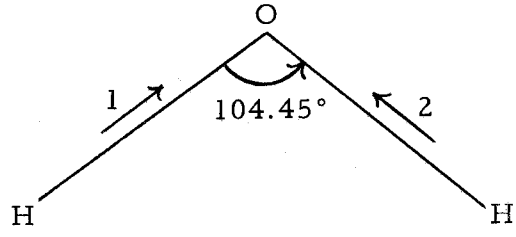

Figure 17. Water reference state.

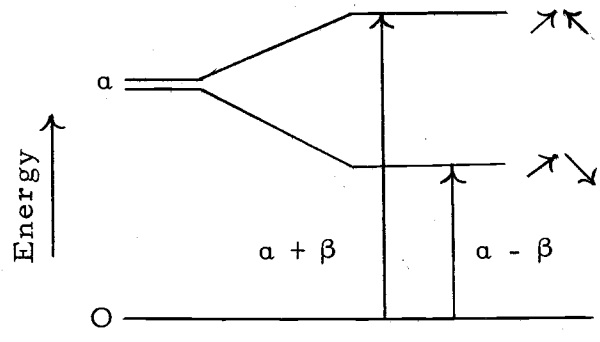

Figure 18. Energy levels diagram for water. The relative phases of the excitations are shown by the arrows.

Calculations of Unperturbed Bond Energies

Extended Huckel Method

The system which concerns us in the next two sections is the chemical bond shown symbolically in Figure 19 below. The letters A and B are at positively charged centers or 'cores', and the e(1) and e(2) are at negatively charged σ bonding electrons. In a CO bond, for example, the cores would be a carbon nucleus surrounded by five electrons and an oxygen nucleus surrounded by seven electrons.

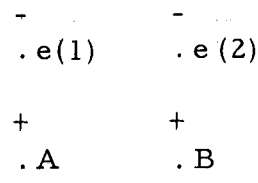

Figure 19. Diagram of the chemical bond.

The extended Huckel theory is simple and practical for semi-quantitative calculations on small polyatomic molecules with σ bond systems. It was first described and used by Hoffmann (17) for hydrocarbons, and has been adapted to many other uses (1, 20, 21, 39).

This method is derived from the variation principle (8, 47), which states that

$$\epsilon_\mu = \frac{\int \psi(\mu) h'_\mu \psi(\mu) d\tau_\mu}{\int \psi(\mu)\psi(\mu) d\tau_\mu} \geq E^0 \tag{15}$$

Here, E^0 is the lowest eigenvalue of the local one electron Hamiltonian

$$h'_\mu = -\frac{\hbar}{2m_e} \nabla^2_{(\mu)} - \frac{e^2}{r_{\mu A}} - \frac{e^2}{r_{\mu B}} + V(\mu) \tag{16}$$

where $V(\mu)$ is an approximation of part of the inseparable electron repulsion term

$$\frac{e^2}{r_{12}} \cong V(1) + V(2) \, . \tag{17}$$

For our two center system we use the LCAO orbitals

$$\begin{aligned} \psi^0 &= \sum_m C_m \chi_m = C_A A + C_B B \\ \psi^+ &= \sum_m C'_m \chi_m = C'_A A + C'_B B \end{aligned} \tag{18}$$

where A and B are valence atomic orbitals for the two centers. The ψ^0 and ψ^+ are respectively the ground and excited state wave functions for the electron. Our problem is to find the set of coefficients which gives the lowest energy for a wave function of this form. To minimize the energy, we set its derivative with respect to each constant equal to zero.

$$\frac{\partial \epsilon}{\partial C_m} = 0 \tag{19}$$

Substituting Equation (18) into (15),

$$\epsilon = \frac{\int (\sum_m C_m \chi_m) h' (\sum_n C_n \chi_n) d\tau}{\int \sum_m C_m \chi_m \sum_n C_n \chi_n d\tau}$$

$$= \frac{\sum_m \sum_n C_m C_n \int \chi_m h' \chi_n d\tau}{\sum_m \sum_n C_m C_n \int \chi_m \chi_n d\tau} . \tag{20}$$

We now wish to introduce some simplification

$$h'_{mn} = \int \chi_m h' \chi_n d\tau \tag{21}$$

and

$$S_{mn} = \int \chi_m \chi_n d\tau \tag{22}$$

The term S_{mn} is called the orbital overlap integral. Equation (20) can now be rearranged to give:

$$\epsilon (\sum_m \sum_n C_m C_n S_{mn}) = \sum_m \sum_n C_m C_n h'_{mn} . \tag{23}$$

The derivative of ϵ with respect to C_m is:

$$\frac{\partial \epsilon}{\partial C_p} \sum_m \sum_n C_m C_n S_{mn} + \epsilon \sum_m C_m S_{mp} + \epsilon \sum_n C_n S_{np} = \sum_m C_m h'_{mp} + \sum_n C_n h'_{np} \cdot \tag{24}$$

Since

$$\frac{\partial \epsilon}{\partial C_p} = 0 \tag{19}$$

and

$$S_{mn} = S_{nm} \tag{25}$$

is always true, and since

$$h'_{mn} = h'_{nm} \tag{26}$$

because h_{mn} is Hermitian, Equation (24) can be reduced to

$$\sum_m C_m (S_{mn} E^0 - h'_{mn}) = 0 \, . \tag{27}$$

This, however, is a set of simultaneous homogeneous equations. They have a solution only if their determinant equals zero. For our specific two center case,

$$\begin{vmatrix} h'_{AA} - E^0 S_{AA} & h'_{AB} - E^0 S_{AB} \\ h'_{BA} - E^0 S_{BA} & h'_{BB} - E^0 S_{BB} \end{vmatrix} = 0$$

Unlike simple Huckel theory, we will not assume that S_{AB} is zero. The quantities h'_{AA} and h'_{BB} were chosen as valence state ionization potentials. The overlap integrals were obtained from integration of Slater atomic orbitals.

We decided to calculate the transition energies for the two series of bonds:

1. CH, NH and OH

2. CC, NC, OC and FC.

We expected that the properties of these bonds would follow trends and thus give an indication of the correct as.

We will determine normalized wave functions for each center in terms of $1\underline{s}(H)$ or hybridized $c_1 2\underline{s}(X) + c_2 2\underline{p}(X)$ functions, where X is either C, N, O or F. Thus, the value of the Coulomb integral h'_{AA} for an $\underline{s}\,\underline{p}^3$ hybridized carbon atom will be:

$$h'_{AA} = \frac{1}{4}(2\underline{s}_A|h'|2\underline{s}_A) + \frac{3}{4}(2\underline{p}_A|h'|2\underline{p}_A) \qquad (28)$$

The numerical value for the energies will be the negative of the valence state ionization potential from the tables of Hinze and Jaffé (16). The wave functions and the valence states used are listed in Table 4.

The overlap integrals S_{mn} are evaluated from the same sets of wave functions. The integrals S_{AA} and S_{BB} are unity since the wave functions are normalized. The S_{AB} integrals are evaluated from the tables of Mullikin et al. (26). For $\underline{s}\,\underline{p}^3$ hybridized CC orbitals, for instance, the overlap integral will have the following form:

$$S_{AB} = (A|B) = ((\tfrac{1}{2})2\underline{s}_A + (\sqrt{3}/2)2\underline{p}_A | (\tfrac{1}{2})2\underline{s}_B + \sqrt{3}/2)2\underline{p}_B)$$

$$= \tfrac{1}{4}(2\underline{s}_A | 2\underline{s}_B) + \sqrt{3}/2(2\underline{s}_A | 2\underline{p}_B) + 3/4(2\underline{p}_A | 2\underline{p}_B) \qquad (29)$$

Each overlap integral is listed in Table 3 with the bond length (3) and orbital exponent used to determine it.

The resonance integral terms h'_{AB} were approximated from an adaptation of Mullikin's approximation (25).

$$h'_{AB} = \frac{K}{2}(h'_{AA} + h'_{BB})S_{AB} \qquad (30)$$

If we let $K = 1$, we have Mullikin's approximation. We use the value $K = 1.3$ from Magnasco's work (20) both because it gives good ground state energies for the CH bond (-15.7797 ev for ethane), and because it gives reasonable transition energies for an isolated CH bond (98.8 kK). In adapting this formula for use with hybridized bonds, we did the hybridization of the bonds first, then substituted in values for the resonance integrals. For example, in a CC bond

$$h'_{AB} = (A|h'|B) = ((\tfrac{1}{2})2\underline{s}_A + (\sqrt{3}/2)2\underline{p}_A | h' | (\tfrac{1}{2})2\underline{s}_B + (\sqrt{3}/2)2\underline{p}_B)$$

$$= \tfrac{1}{4}(2\underline{s}_A | h' | 2\underline{s}_B) + \sqrt{3}/2(2\underline{s}_A | h' | 2\underline{p}_B) + 3/4(2\underline{p}_A | h' | 2\underline{p}_B) \qquad (31)$$

Now the individual terms, such as the $(2\underline{s}_A | h' | 2\underline{s}_B)$, are evaluated from Equation (28) with the appropriate valence state ionization potentials and overlap integrals from Table 3.

Table 3. Overlap integrals with bond lengths and orbital exponents used to calculate them.

Bond	Bond Length in Å (3)	Orbital Exponents	Atomic Orbitals	Overlap Integral
CH	1.10	1.20 (H)	1s(H)-2s(C)	.514
		1.625 (C)	1s(H)-2p(C)	.484
NH	1.00	1.20 (H)	1s(H)-2s(N)	.512
		1.95 (N)	1s(H)-2p(N)	.438
OH	0.96	1.20 (H)	1s(H)-2s(O)	.478
		2.275 (O)	1s(H)-2p(O)	.382
CC	1.54	1.625 (C)	2s(C)-2s(C)	.341
			2s(C)-2p(C)	.365
			2p(C)-2p(C)	.329
CN	1.47	1.625 (C)	2s(C)-2s(N)	.308
		1.95 (N)	2s(C)-2p(N)	.303
			2p(C)-2s(N)	.372
			2p(C)-2p(N)	.313
CO	1.43	1.625 (C)	2s(C)-2s(O)	.274
		2.275 (O)	2s(C)-2p(O)	.246
			2p(C)-2s(O)	.358
			2p(C)-2p(O)	.283
CF	1.35	1.625 (C)	2s(C)-2s(F)	.262
		2.60 (F)	2s(C)-2p(F)	.214
			2p(C)-2s(F)	.361
			2p(C)-2p(F)	.261

Once these integrals have been determined, they are inserted into the determinant of Equation (27) which is solved for both roots. The lowest, or most negative value, is the calculated ground state bond energy. The highest, or least negative root, is the theoretical excited state energy.

Table 4. Hybrid wave functions and valence states used in Huckel calculations.

Atom	Hybrid Wave Function	Valence State
Method A		
H	$1\underline{s}$	$\underline{s}$
C	$\frac{1}{2}(2\underline{s}) + \sqrt{3}/2(2\underline{p})$	$\underline{s}\ \underline{p}\ \underline{p}\ \underline{p}$
N	$2\underline{p}$	$\underline{s}^2\ \underline{p}\ \underline{p}\ \underline{p}$
O	$2\underline{p}$	$\underline{s}^2\ \underline{p}^2\ \underline{p}\ \underline{p}$
F	$2\underline{p}$	$\underline{s}^2\ \underline{p}^2\ \underline{p}^2\ \underline{p}$
Method B		
H	$1\underline{s}$	$\underline{s}$
C	$\frac{1}{2}(2\underline{s}) + \sqrt{3}/2(2\underline{p})$	$\underline{s}\ \underline{p}\ \underline{p}\ \underline{p}$
N	$1/\sqrt{5}(2\underline{s}) + 2/\sqrt{5}(2\underline{p})$	$\underline{s}\ \underline{p}^2\ \underline{p}\ \underline{p}$
O	$1/\sqrt{6}(2\underline{s}) + (5/6)^{1/2}(2\underline{p})$	$\underline{s}\ \underline{p}^2\ \underline{p}^2\ \underline{p}$
F	$1/\sqrt{7}(2\underline{s}) + (6/7)^{1/2}(2\underline{p})$	$\frac{1}{7}\underline{s}\ \underline{p}^2\ \underline{p}^2\ \underline{p}^2$ $+\frac{6}{7}\underline{s}^2\ \underline{p}^2\ \underline{p}^2\ \underline{p}$
Method C		
H	$1\underline{s}$	$\underline{s}$
C	$\frac{1}{2}(2\underline{s}) + \sqrt{3}/2(2\underline{p})$	$\underline{te}\ \underline{te}\ \underline{te}\ \underline{te}$
N	$\frac{1}{2}(2\underline{s}) + \sqrt{3}/2(2\underline{p})$	$\underline{te}^2\ \underline{te}\ \underline{te}\ \underline{te}$
O	$\frac{1}{2}(2\underline{s}) + \sqrt{3}/2(2\underline{p})$	$\underline{te}^2\ \underline{te}^2\ \underline{te}\ \underline{te}$
F	$\frac{1}{2}(2\underline{s}) + \sqrt{3}/2(2\underline{p})$	$\frac{1}{4}\underline{s}\ \underline{p}^2\ \underline{p}^2\ \underline{p}^2$ $+\frac{3}{4}\underline{s}^2\ \underline{p}^2\ \underline{p}^2\ \underline{p}$

Their difference,

$$E(\text{excited}) - E(\text{ground}) = \Delta E\, \sigma - \sigma^{*} = a \tag{32}$$

is the transition energy for one of the electrons in the isolated bond.

The energy calculations for the series of bonds were carried out with three different sets of atomic wave functions. There is some controversy concerning the hybridization of the N, O and F atoms in molecules. The observed bond angle for water is 104.45°, while for ammonia it is 107.3°. These angles are nearly as large as the HCH bond angle in methane, which implies that water and ammonia, too, are hybridized tetrahedral. According to Pauling (31, page 111) the angles are larger than 90° (expected for pure 2p orbitals) because of charge repulsion. The hydrogens become partially positively charged and thus repel each other. Later in a discussion of ammonia (30, pages 164-165) he claims that the three NH bonds each have about 93% 2p character with the remaining 7% in 2s character. Thus, we were unable to decide whether to use pure 2p orbitals for the N, O and F atoms, or to use sp^3 hybridized orbitals for N and O.

Since we could not be sure of the right orbital wave function, we adopted the safest approach, which was to try three different methods of hybridization. We called the methods A, B and C. In all the methods we used 1s orbitals for hydrogen. For methods A and B, we used the sp^3 hybrid orbital for the carbon. In method A the N, O

and F atoms were all considered to have pure 2p orbitals. For method B, we took the one electron in the 2s orbital in the hybridized valence state divided by the total number of outer shell electrons, as the percentage of 2s character for the bond. The rest of the orbital was considered 2p character. For method C, sp^3 hybridization (tetrahedral) was chosen for all orbitals. However, Hinze and Jaffé (16) do not give a tetrahedral ionization potential for F. Here we take it to be 1/4 of the energy in the $sp^2p^2p^2$ valence state plus 3/4 of the energy of the $s^2p^2p^2p$ valence state. For method C all the overlap integrals were calculated from the sp^3 type wave functions. The valence states and wave functions are listed in Table 4 for methods A, B and C. The method B wave functions represent a compromise between two choices which we feel are both too extreme. Klessinger (19) treated the same series of bonds in a very similar way.

The results of these calculations are listed in Table 5. For methods A and B, the σ-σ^* transition energies for CH and CC bonds are almost degenerate at 100 kK.

In method A all the other energies are considerably lower than 100 kK. Since methane, CH_4, has a much lower first transition band at 76 kK (6) than carbon tetrafluoride at about 111 kK (4), it is clear that the results of method A are wrong for CF bonds. Noting the value of 46 kK for OH, we recall that H_2O will be predicted in

independent systems theory to have a first transition at $\lambda = (46-\beta)$ kK, or somewhat lower than 46 kK. Since water vapor has its lowest energy peak at 60 kK, the prediction is poor again. For these reasons, we had no confidence in method A.

Table 5. Summary of Huckel results for calculation of the $\sigma - \sigma^*$ transition energies in kK.

Bond	Method	Energy in kK A	B	C
CH		98.83	98.83	85.75
NH		36.24	102.77	100.65
OH		46.32	119.62	131.28
CC		102.70	102.70	79.01
CN		40.12	100.48	88.70
CO		47.22	115.29	118.62
CF		70.00	120.90	119.54

For methods B and C, all the transitions are either higher than the CH or CC energies or at least degenerate with them. Note that in energy, CN < CO < CF and NH < OH in all cases. The CH and CC transitions are slightly lower than experimental results indicate in method C. The results of method B appear to be the most closely related to the experimental results.

Complete Neglect of Differential Overlap

Although the Huckel method is easy to use, it has some disadvantages in that it does not treat electron repulsion explicitly. To

describe the system more accurately, the Hamiltonian should include all the electrons in the two atoms with the interelectronic repulsions included. An apparently more reasonable approach is the ab initio calculations of Goeppert-Mayer and Sklar (9) on the first excited levels of benzene using only the six pi electrons and based on a single configuration wave function.

A simplified theory has been developed by Pople (33) for pi electron systems with complete neglect of differential overlap (CNDO). This was later generalized to σ electron systems by Pople, Santry and Segal (34, 35, 36). This method will be adapted in this work for use with the localized bond system illustrated in Figure 19.

The complete two electron Hamiltonian which describes this system is the following:

$$h = -\frac{\hbar^2}{2m_e}(\nabla^2(1)+\nabla^2(2)) - \frac{e^2}{r_{1A}} - \frac{e^2}{r_{1B}} - \frac{e^2}{r_{2A}} - \frac{e^2}{r_{2B}} + \frac{e^2}{r_{12}} \qquad (4)$$

where the indices A and B represent the two centers, and 1 and 2 the two electrons. The factor m_e is the mass of an electron and the $\hbar$ is Plank's constant divided by 2π.

In order to present our derivation of the equation describing the $\sigma - \sigma^*$ transition energies for this system, we will define abbreviated Hamiltonians and wave functions which describe our particular system. Let

$$h = h'_{core} + \frac{e^2}{r_{12}} \tag{33}$$

where e^2/r_{12} is the electrostatic repulsion between the two σ electrons and

$$h'_{core} = h_{core}(1) + h_{core}(2) \tag{34}$$

with, for instance,

$$h_{core}(1) = -\frac{\hbar^2}{2m_e}\nabla^2(1) - \frac{e^2}{r_{1A}} - \frac{e^2}{r_{1B}} . \tag{35}$$

The first term in this equation represents the kinetic energy of the AB^{+2} system for electron (1) and the last two terms are its potential energy in the field of AB^{+2}.

The two wave functions which describe this system are normalized antisymmetrized product functions. For the ground state

$$\phi^0 = \frac{1}{\sqrt{2}}\psi^0(1)\psi^0(2)(\alpha(1)\beta(2) - \beta(1)\alpha(2)) \tag{36}$$

where, for electron (μ), the molecular orbitals are approximated as linear combinations of atomic orbitals (LCAO).

$$\psi^0(\mu) = (C_A A + C_B B)(\mu) \tag{37}$$

The symbols A and B are for valence Slater atomic orbitals for

the two different centers described by Figure 19. The spin functions, α and β, are orthonormal by definition. The two constants, C_A and C_B, are the normalization constants from the ground state energy from extended Huckel method.

Since the two electrons are in a closed shell in the ground state, there is only one allowed ground state in which the electrons can have opposite spin functions. There are four allowed first excited states, however, since the two electrons are in different levels in this case (see Figure 20 below) and the electrons no longer need to have opposite spin functions.

There are four different wave functions which are antisymmetric with respect to electron exchange for the excited state

$$\phi^+ = \frac{1}{2}[\psi^0(1)\psi^+(2)+\psi^+(1)\psi^0(2)][\alpha(1)\beta(2)-\beta(1)\alpha(2)] \qquad (38)$$

and

$$\phi^1 = \frac{1}{2}[\psi^0(1)\psi^+(2)-\psi^+(1)\psi^0(2)][\alpha(1)\alpha(2)]$$

$$\phi^2 = \frac{1}{2}[\psi^0(1)\psi^+(2)-\psi^+(1)\psi^0(2)][\beta(1)\beta(2)] \qquad (39)$$

$$\phi^3 = \frac{1}{2}[\psi^0(1)\psi^+(2)-\psi^+(1)\psi^0(2)][\alpha(1)\beta(2)+\beta(1)\alpha(2)]$$

The meaning of ψ^0 remains unchanged;

$$\psi^+(\mu) = (C'_A A + C'_B B)(\mu) \; . \qquad (40)$$

The normalization coefficients, C'_A and C'_B, are obtained from the excited state energy of the extended Huckel method. Note that the first equation has a different orbital wave function from the last three. The last three equations all have the same energy associated with them and are said to describe a triplet state. The first equation has a different energy and is said to be a singlet state.

The excited state which we observe in the vacuum ultraviolet spectra discussed earlier is a singlet state. Therefore we wish to use the wave function described in Equation (38).

To obtain the ground state energy, we perform the following operation

$$E^0 = (\phi^0|h|\phi^0) \tag{41}$$
$$= \frac{1}{2}(\psi^0(1)\psi^0(2)(\alpha(1)\beta(2)-\beta(1)\alpha(2))|h|\psi^0(1)\psi^0(2)(\alpha(1)\beta(2)-\beta(1)\alpha(2))$$

Omitting terms in which the spins are orthogonal and simplifying, we arrive at the following:

$$E^0 = (\psi^0(1)\psi^0(2)|h|\psi^0(1)\psi^0(2)) \tag{42}$$

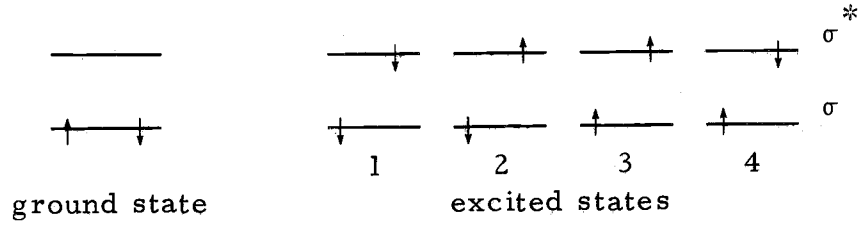

Figure 20. Allowed states for two electron system. Arrows indicate relative spin phase, i.e., +1/2 or -1/2.

Substituting in the definition of h'_{core} in Equation (34) and the linear combination atomic orbitals in Equation (37) and combining equivalent terms, we obtain:

$$\begin{aligned} E^0 = {} & C_A^2(A(1)A(2)|h'_{core}|A(1)A(2)) + 2C_AC_B(A(1)A(2)|h'_{core}|B(1)B(2)) \\ & + C_B^2(B(1)B(2)|h'_{core}|B(1)B(2)) + C_A^4(AA|AA) + 4C_A^3C_B(AA|AB) \\ & + 4C_A^2C_B^2(AB|AB) + 4C_AC_B^3(AB|BB) + C_B^4(BB|BB) \\ & + 2C_A^2C_B^2(AA|BB) . \end{aligned} \tag{43}$$

The integrals $(AA|BB)$ etc. represent interelectronic repulsion energies, i.e., $(A(1)A(1)|\frac{e^2}{r_{12}}|B(2)B(2))$. One calculates the excited state energy in a similar way, from the wave function in Equation (38)

$$\begin{aligned} E^+ &= (\phi^+|h|\phi^+) \\ &= \frac{1}{4}\,((\psi^0(1)\psi^+(2)+\psi^+(1)\psi^0(2))(\alpha(1)\beta(2)-\beta(1)\alpha(2)) \\ &\qquad |h|(\psi^0(1)\psi^+(2)+\psi^+(1)\psi^0(2))(\alpha(1)\beta(2)-\beta(1)\alpha(2))\,) \end{aligned} \tag{44}$$

The solution is parallel to that in Equation (43), but is so complex that we will not expand it here.

Instead, we introduce the first three CNDO approximations of Pople, Santry and Segal (34). These approximations make the equation for the excited state much simpler. Following this we

calculate the simplified excited state energy as well as the isolated bond transition energy. Next we introduce the last two of the five CNDO approximations. Finally, we explain how the integrals in the energy equation were evaluated.

The first approximation treats valence atomic orbitals, such as A and B, as an orthonormal set. Thus, the overlap S_{AB} has no value.

The second approximation is similar. It allows neglect of interelectronic repulsion integrals which depend on overlapping charge densities of different basis orbitals. Thus, the integrals $(AB|AA)$ and $(AB|AB)$ etc. will be ignored. We are left with only three non-zero repulsion terms: $(AA|AA)$, $(AA|BB)$ and $(BB|BB)$.

The third approximation states that the interelectronic repulsions depend only on the center, A or B, to which the electron belongs, rather than to any specific orbital. This approximation was made so that Pople could perform transformations on the molecular electron repulsion integrals and still obtain the same results as discussed under approximation two. This forced them to use s functions. In the present calculations of localized bond energies, the problem of transformations did not arise. Instead, we used hybridized wave functions for all centers except hydrogen. These are simply represented by 'A' and 'B', which is essentially the same as making this approximation.

Applying the first and second approximations to Equation (44) for the excited state energy of the bond AB, we obtain

$$
\begin{aligned}
E^{+} = & \frac{1}{2}(C_A^2+C_A'^2)(A(1)A(2)|h'_{core}|A(1)A(2)) \\
& + (C_A C_B + C'_A C'_B)(A(1)A(2)|h'_{core}|B(1)B(2)) \\
& + \frac{1}{2}(C_B^2+C_B'^2)(B(1)B(2)|h'_{core}|B(1)B(2)) + 2C_A'^2 C_A^2 (AA|AA) \\
& + (C_B^2 C_A'^2 + C_A^2 C_B'^2 + 2C_A C'_A C_B C'_B)(AA|BB) + 2\, C_B^2 C_B'^2\, (BB|BB).
\end{aligned}
\tag{45}
$$

The localized bond transition energy which we wish to calculate here is simply the difference between the ground and first excited states.

$$
\begin{aligned}
\Delta E_{\sigma-\sigma^*} = & \frac{1}{2}(C_A'^2 - C_A^2)(A(1)A(2)|h'_{core}|A(1)A(2)) \\
& + (C'_A C'_B - C_A C_B)(A(1)A(2)|h'_{core}|B(1)B(2)) \\
& + \frac{1}{2}(C_B'^2 - C_B^2)(B(1)B(2)|h'_{core}|B(1)B(2)) + (2C_A'^2 C_A^2 - C_A^4)(AA|AA) \\
& + (2C_B C'_B C_A C'_A + C_B^2 C_A'^2 + C_A^2 C_B'^2 - 2C_A^2 C_B^2)(AA|BB) \\
& + (2C_B^2 C_B'^2 - C_B^4)(BB|BB)
\end{aligned}
\tag{46}
$$

Though this equation looks complex, it actually contains only four different kinds of integrals. Inserting h_{core} as defined in Equation (35) into the first term:

$$(A(\mu)|h_{core}(\mu)|A(\mu)) = (A|-\frac{1}{2}\nabla^2 - \frac{e^2}{r_{1A}}|A) - (A|\frac{e^2}{r_{1B}}|A) \tag{47}$$

$$= U_{AA} - (A|\frac{e^2}{r_{1B}}|A) .$$

The first term, U_{AA}, includes the kinetic energy of one electron in orbital A, plus the energy of attraction between that electron and the center A. This integral can be evaluated theoretically from approximate atomic orbitals, or empirically from experimental data. The second term describes the energy of attraction between one electron in an atomic orbital on center A and the charged core at B.

The fourth CNDO approximation states that this attraction integral would not have a value if two different orbitals on center A had been used. In our case it does have a value, since the orbitals are on different centers. We made the approximation by defining the wave function as "A" and "B".

The fifth CNDO approximation states that:

$$(A(\mu)|h_{core}(\mu)|B(\mu)) = \beta_{AB} = \beta^0_{AB} S_{AB} \tag{48}$$

where β^0_{AB} is an energy depending only on the properties of the two centers A and B. Pople's group did not attempt to calculate this, but fitted values to LCAO-self consistent field calculations on some

diatomic molecules. We obtain this value from another method which is described below. The value S_{AB} is the usual orbital overlap integral.

We evaluated $E_{\sigma-\sigma^*}$ for the series of bonds two separate times. The first calculation was carried out with a semiempirical set of integrals, the second one was done with completely empirical integrals. In both sets of calculations, the constants C_A, C'_A, C_B and C'_B, and the wave functions, were taken from Huckel method B. The parameter β^0_{AB} was obtained from the same source with the value of $0.65\ (I_A+I_B)$. The differences between the two calculations were primarily in the method of obtaining the interelectronic repulsion terms, $(AA|AA)$ and $(AA|BB)$.

The one center electron repulsion integral was first calculated from Slater atomic orbitals (24) and second from the empirical method of Pariser (16, 29).

$$(AA|AA) = I_A - A_A \tag{49}$$

where A_A is the electron affinity of center A and I_A is its valence state ionization potential.

The two center electron repulsion integrals were also first calculated from atomic orbitals (41), then from an empirical method of Mataga et al. (22, 28). In the case of a CC bond, with R as

internuclear distance in atomic units,

$$(AA|BB) = \frac{1}{R+a_A} \tag{50}$$

$$(AA|AA) = \frac{1}{a_A} = I_A - A_A \tag{51}$$

In the case of a heteropolar bond, we would use arithmatic averages of the values of a.

Finally we evaluated the $(A|h_{core}|A)$ terms. The one center part, called U_{AA} (see Equation (47)), was approximated by Pople to be

$$U_{AA} = -\frac{1}{2}(I_A+A_A) - (Z_A-\frac{1}{2})(AA|AA) \tag{52}$$

Where Z_A is the core charge on center A, which is unity in this case. If formula (49) is substituted into (52), we can arrive at:

$$U_{AA} = -I_A . \tag{53}$$

It seemed more reasonable to use this approximation throughout, than to have U_{AA} itself one-half empirical and one-half theoretical. The two center part, $(A|\frac{e^2}{r_{1B}}|A)$, of Equation (47) was approximated by Pople (36) as:

$$(A|\frac{e^2}{r_{1B}}|A) = Z_B(AA|BB) \tag{54}$$

with Z_B the core charge on center B, which was unity. Because

of this approximation, the value of $(A|h_{core}|A)$ varied depending on whether the two center electron repulsion integrals were obtained empirically or theoretically.

The results of these two sets of calculations are given in Table 6. These describe a situation in which the field of the core is independent of its neighboring atoms. This was much simpler than a self-consistent field calculation would have been. It was thought that the more complex calculation would not have been any more precise than the simpler method, since so many approximations were made in the values of the integrals.

Table 6. Complete neglect of differential overlap results for the $\sigma - \sigma^*$ transition energies in kK.

Bond	Method	Energy	
		Semi-Empirical[1]	Completely Empirical[2]
CH		73.39	126.24
NH		109.98	132.53
OH		154.82	151.40
CC		122.12	144.32
CN		149.67	141.87
CO		152.66	145.32
CF		135.30	130.10

[1] $(AA|AA)$, $(AA|BB)$ are calculated theoretically.

[2] $(AA|AA)$, $(AA|BB)$ are taken from experiment.

In the present results, there is no longer the degeneracy between the CH and CC bond transition energies. In the first set of energies,

where the integrals used were only partly empirical, the transition energy for the CH bond is lower than any experimental peak in methane. But with the exception of the CF bond, the energy trends seen here are the same as that of method C in the Huckel calculation. All the energies in the totally empirical method are much higher than in the extended Huckel calculation. The set CH, NH and OH show the same energy trend as do all the other methods, but in the CC, CN, CO and CF set, all the energies have about the same value. As a result of these five sets of energies, we can feel confident that the isolated bond transition energies are not lower for the OH or the CO bonds of the model sugars than for the CH and CC bonds of the alkanes.

Nearest Neighbor Interaction Energies

The bond energies which we have now calculated provide the diagonal elements of the independent systems determinants. In order to calculate electronic transitions for a molecular system, we also need the off-diagonal elements, or interaction energies. These elements, called β_{ij}, are defined in Equation (12). In the present work, only interactions for nearest neighbor bonds will be considered.

We cannot calculate β_{ij} directly. We approximate it as the electrostatic interaction between transition moments. We calculate the energy of interaction using Coulomb's law directly. The system

which we are considering is shown in Figure 21.

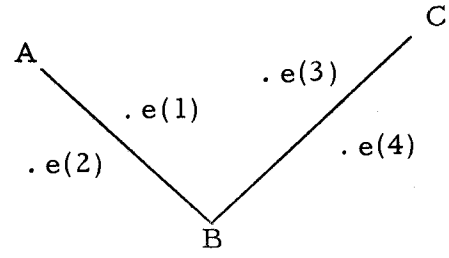

Figure 21. Nearest neighbor bond system. A, B and C are atomic centers. The $e(\mu)$ are the four σ bonding electrons.

This method requires the knowledge of the transition moment $\mu_{AB}(\mu\nu)$ which is physically visualized as a separation of charge in the excited bond.

$$\mu_{AB} = (\phi^{+}_{AB}(\mu, \nu) | \vec{er}(\mu, \nu) | \phi^{0}_{AB}(\mu, \nu)) \tag{56}$$

Unfortunately, it is not easy to know these quantities exactly for all the bonds under consideration. The values can be determined experimentally from the integrated intensity of the $\sigma - \sigma^{*}$ transition band by the relationship:

$$\mu_{AB} = (9.15 \times 10^{-18} \int \epsilon d\bar{\nu})^{1/2} \tag{57}$$

where $\bar{\nu}$ is the frequency $(1/\lambda)$ in wave numbers. This, however, can only be used for bonds whose $\sigma - \sigma^{*}$ transition energies are known experimentally. We cannot use this method for the μ_{OH}

or μ_{CO}. Another experimental method is to use the interaction energy, β_{ij}, calculated from the independent systems method in the next section to find μ_{CH}, μ_{CC} and μ_{CF} by trial and error in the monopole approximation. This was carried out, but still could not, of course, give μ_{OH} or μ_{CO}.

Finally, we can calculate any transition moment from the Slater atomic orbitals. Transition moments for all the bonds under consideration were calculated in this way. Using antisymmetrized product functions given in Equations (36) and (38) in the equation for the transition moment, μ_{AB} (56), we obtain

$$\mu_{AB} = \sqrt{2}\,(C'_A A + C'_B B | \vec{r} | C_A A + C_B B)$$

$$= \sqrt{2}[C'_A C_A\,(A|\vec{r}|A) + C'_B C_B\,(B|\vec{r}|B) + (C'_B C_A + C'_A C_B)\,(A|\vec{r}|B)] \qquad (57)$$

The three different integrals involved here correspond to one and two center dipole moments which can be evaluated from the wave functions (24, page 37).

The results of this calculation are given in Table 7. The constants used in this calculation were taken from method B of the Huckel calculation. The two center dipole moments for the CN, CO and CF bonds were very small and very difficult to calculate, so these were omitted from the value of the transition moment.

Table 7. Calculation of the energies of interaction for the bond series. $\beta_{AB,BC}$ are for like bonds.

Bond	$\mu_{calculated}$	R_{AB} in Å	$\beta_{independent\ systems\ (experimental)}$	$\mu_{independent\ systems}$	$\frac{\mu_{calculated}}{\mu_{independent\ systems}}$	$\beta_{independent\ systems\ (fitted)}$
CH	1.06	1.10	18.6	.18	5.9	18.6
NH	0.956	1.00		.16	5.9	21.0
OH	0.765	0.96		.13	5.9	14.4
CC	1.43	1.54	26.4	.35	4.1	26.4
CN	1.22	1.47		.30-.21	4.1-5.7	22.1-9.6
CO	0.914	1.43		.22-.16	4.1-5.7	12.4-6.1
CF	0.741	1.35	6.5	.13	5.7	6.5

The Coulomb interaction was carried out as illustrated in Figure 22. The theoretical transition moments were used at first, but they gave $\beta_{AB,BC}$ values that were even larger than the α_{AB} matrix elements had been. These were obviously about ten times too large. Therefore, we decided to take experimental values of $\beta_{AB,BC}$ for CF, CC and CH bonds, which were found in the next section, to estimate the value of the transition moment. We hoped that the experimental values of the transition moments would differ from the theoretical values by a constant factor. This factor could then be used to estimate the experimental values for the rest of the bonds under consideration. As shown in Table 7, the factor turned out to be quite different for μ_{CC} than for μ_{CF} and μ_{CH}. It is shown in the next section that the CC bond transition energy was too low for the Huckel method B. Thus, it is not surprising that the transition moment calculated from its results is also too low. Our ability to calculate the transition moment is limited by our knowledge of the normalized ground and excited state wave functions.

The theoretical transition moments for the CO and OH bonds must be too large by a similar amount. We decided that the NH and OH transition moments were probably too large by the same factor as the μ_{CH}. For μ_{CN} and μ_{CO}, the factor could be as small as in μ_{CC} or as large as in μ_{CF}. We decided to use both factors for these two to give a range of values. We are ultimately interested

$$\beta = 2 \times 116\left(\frac{1}{r_{++}} + \frac{1}{r_{--}} - \frac{2}{r_{+-}}\right)$$

$$= 232\left(\frac{1}{.882} + \frac{1}{.670} - \frac{2}{.780}\right)$$

$$= 232(.0622)$$

$$= 14.4 \text{ kK}$$

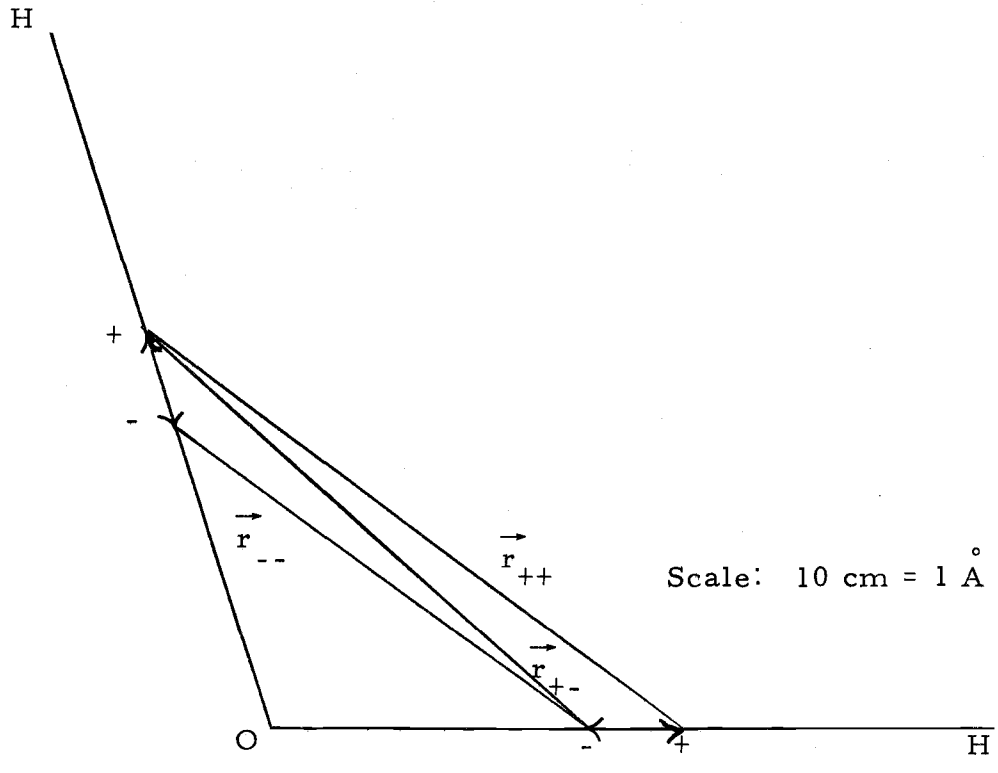

Figure 22. Method for calculating matrix elements of β using scale drawing.

in the $\sigma - \sigma^*$ transitions which the independent systems method predicts for model sugars. Since the transitions will have lower energies if the $\beta_{CO,CO}$ is a larger number, we wish to show that even the largest μ_{CO} allows us to conclude that the low energy bands are $n - \sigma^*$ transitions. Table 7 shows that when we use the larger value for μ_{CN} and μ_{CO}, the predicted values for $\beta_{CO,CO}$ and $\beta_{CN,CN}$ are still smaller than the value for $\beta_{CC,CC}$.

The only values for $\beta_{AB,BC}$ which were calculated in this way were for interactions of like bonds. For dissimilar bond interactions, the energies were estimated as the square root of the products of the appropriate energies given in Table 7.

Independent Systems Calculation

We determined the isolated bond transition energies and interaction energies for the CH, CC and CF bonds from experiment (6, 38). Since CF_3H has its lowest peak at 87 to 88.5 kK, we know that the transition energy for the CH bond is greater than 88.5 kK. Noting that the compounds CH_2F_2, CH_3F and CH_4 all have peaks at $\alpha_{CH} - \beta_{CH,CH} = 77$ kK, we find that the CH, CH interaction energy must be at least 11.5 kK.

Carbon tetrafluoride, CF_4, has its first peak at 111 kK (4). Thus, the isolated CF bond must have a transition energy greater than 111 kK.

The transition energy of the CC bond is determined from the spectra of ethane and propane. Ethane has a CC transition at 74 to 77 kK, while propane has two CC transitions. Propane has one peak at 71 to 73 kK and another at 77 to 79.5 kK, with a splitting of about 6 kK.

The independent systems calculations were originally carried out with the transition energies calculated in Huckel method B. Here the energies for α_{CC} and α_{CH} are almost degenerate at about 100 kK. These values did not fit the experimental data in that the propane splitting could not be made large enough without pushing the peaks to low energies (see Table 8). This table indicates that the propane splitting can be increased by increasing $\beta_{CC, CC}$.

Table 8. Positions of peaks and splittings for ethane and propane in kK with increasing β_{CC}.

α_{CC}	α_{CH}	β_{CC}	β_{CH}	Et	Pr_1	Pr_2	CH	Split
102.7	98.8	20	20	68.5	66.2	71.2	78.8	5.1
102.7	98.8	15	20	75.4	74.3	76.5	78.8	2.2

However, it is shown in Table 9 that increasing α_{CH} and the corresponding $\beta_{CH, CH}$ to continue to fit methane, results in a lowering of the propane splitting as well as lowering the energy of the CC bond transition. For this reason, it seemed advisable to keep α_{CH} as small as possible.

Table 9. Positions and splittings for peaks of ethane and propane in kK with increasing α_{CH} and β_{CH}.

α_{CC}	α_{CH}	β_{CC}	β_{CH}	Et	Pr_1	Pr_2	CH	Split
109	107	19	29	74.1	72.8	75.4	78	2.6
109	109	19	31	73.5	72.4	74.7	78	2.3

It was noted that under the condition of α_{CH} being around 100 kK, and α_{CC} 102 kK or larger, it is necessary that the $\beta_{CC,CC}$ be 18 kK or greater in order to get a sufficiently large propane CCC splitting. When α_{CC} is low, the high $\beta_{CC,CC}$ causes the CC transitions to be at low energies. An increase in α_{CC} raises the CC transitions, but lowers the propane splitting (see Table 10). This suggests a further increase in the $\beta_{CC,CC}$.

Table 10. Positions of peaks and splittings for ethane and propane in kK with increasing α_{CC}.

α_{CC}	α_{CH}	β_{CC}	β_{CH}	Et	Pr_1	Pr_2	CH	Split
105	105	20	28	67.9	66.7	69.7	77	3
110	105	20	28	71.9	70.8	72.9	77	1.6

These trends indicate that the empirical values for α_{CC}, α_{CH}, $\beta_{CH,CH}$ and $\beta_{CC,CC}$ given by Raymonda (37) and listed in Table 11 are unique. The relationship between the α_{CC} and α_{CH} is the same as that in the completely empirical CNDO calculations.

Table 11. Positions of peaks and splittings for ethane and propane in kK.

α_{CC}	α_{CH}	β_{CC}	β_{CH}	Et	Pr_1	Pr_2	CH	Split
120	95.6	26.4	17.6	75.6	72.6	77.6	78	5

When the fluoromethanes were adapted to these results, it was found that the CH transition was slightly too high. When the CH transition was lowered to 77 kK by increasing $\beta_{CH,CH}$ to 18.6 kK, we were able to reproduce the experimental results (see Figure 26 and Table 12). It is interesting to note that this α_{CF} is in the same relationship to α_{CC} as it was in the completely empirical CNDO calculation.

Table 12. Lowest calculated transition energies for fluoromethanes in kK.

α_{CH}	α_{CF}	β_{CH}	β_{CF}	CF_4	CF_3H	CF_2H_2	CFH_3	CH_4
95.6	117.5	18.6	6.5	111	87.3	77.0	77.0	77.0

Finally, we wondered whether there might be more sets of α's and β's for the CH, CC and CF bonds at higher energies. To determine this we carried out independent systems calculations for propane with α_{CH} set at 105 kK and with $\beta_{CH,CH}$ at 28 kK. The value of α_{CC} was varied between 125 and 155 kK. The value of $\beta_{CC,CC}$ was also varied to get a range of CCC splitting at each

energy. It was found that whenever the splitting was sufficiently large, the average energy of the transition was too low (see Figure 25). Since we could not fit the $\alpha_{CH} = 105$ kK value to the propane, we assume that the value $\alpha_{CH} = 95.6$ kK is unique for the hydrocarbons.

The experimental spectra of the hydrocarbons ethane, propane, butane, cyclopentane and methylcyclopentane (38) are presented in Figures 23 and 24 with the predicted transitions calculated as described earlier. It is encouraging to note that the transitions are predicted very well in all of these spectra.

We now felt prepared to undertake the calculations of the $\sigma - \sigma^*$ transitions of the model sugar compounds. The previous results indicate that the completely empirical CNDO calculations are a fairly good way to calculate the relative transition energies for the bonds. Therefore, we concluded that the $\sigma - \sigma^*$ transition spectra for the model sugar compounds could most accurately be estimated from the hydrocarbon α, β values, with the addition of $\alpha_{CO} = 120$ kK and $\alpha_{OH} = 120$ kK. This case would predict the reddest transitions. The values for the bond interactions were set at $\beta_{CO, CO} = 26.4$ kK and $\beta_{OH, OH} = 18.6$ kK. The results of calculations for some hydrocarbons and model sugar compounds are compared with experiment in Figure 27. For the experimental results, we could easily denote individual peaks in the low energy region, but could not really

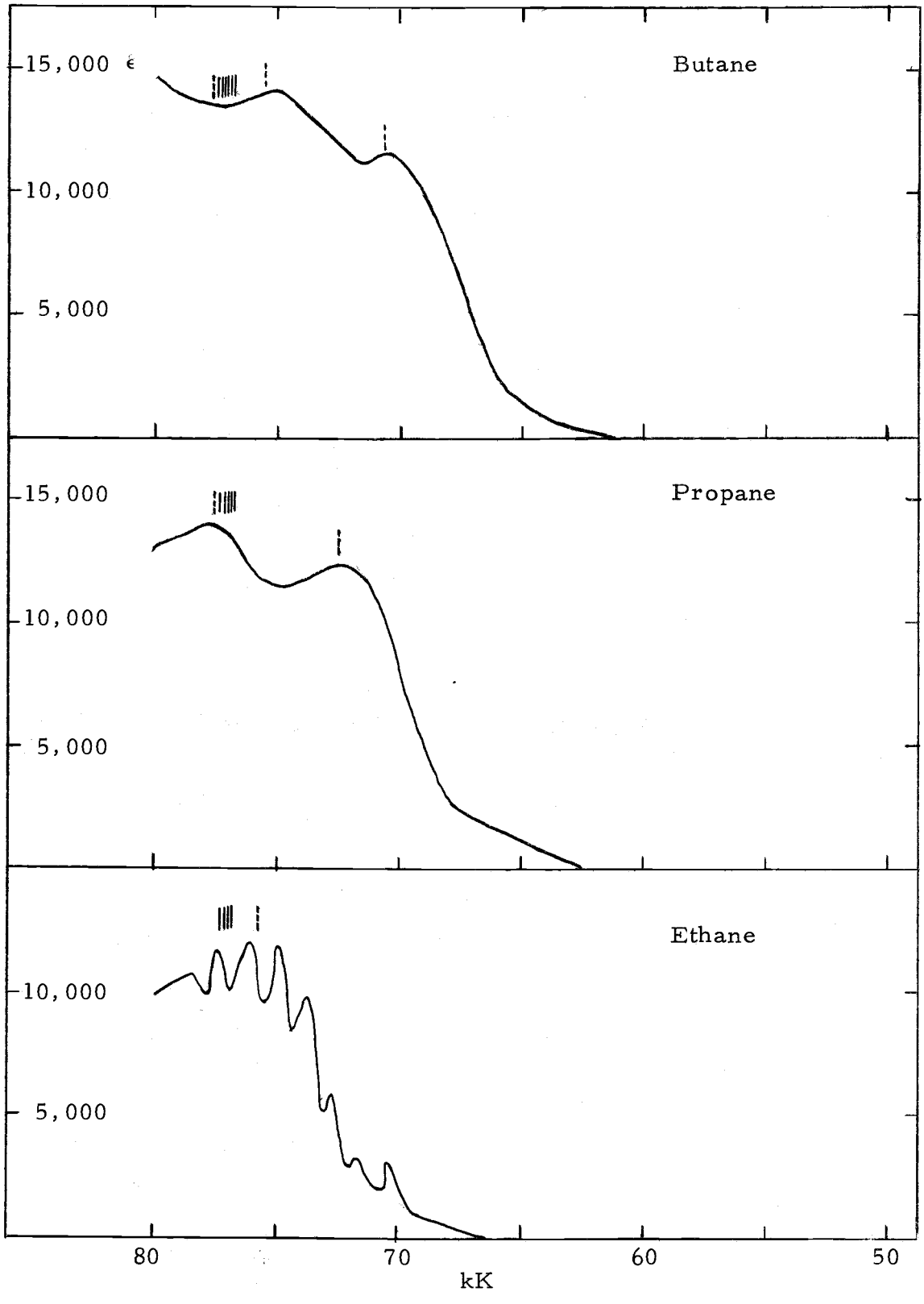

Figure 23. Spectra of alkanes with predicted peaks. The solid lines are CH transitions, the dashed lines are both CH and CC.

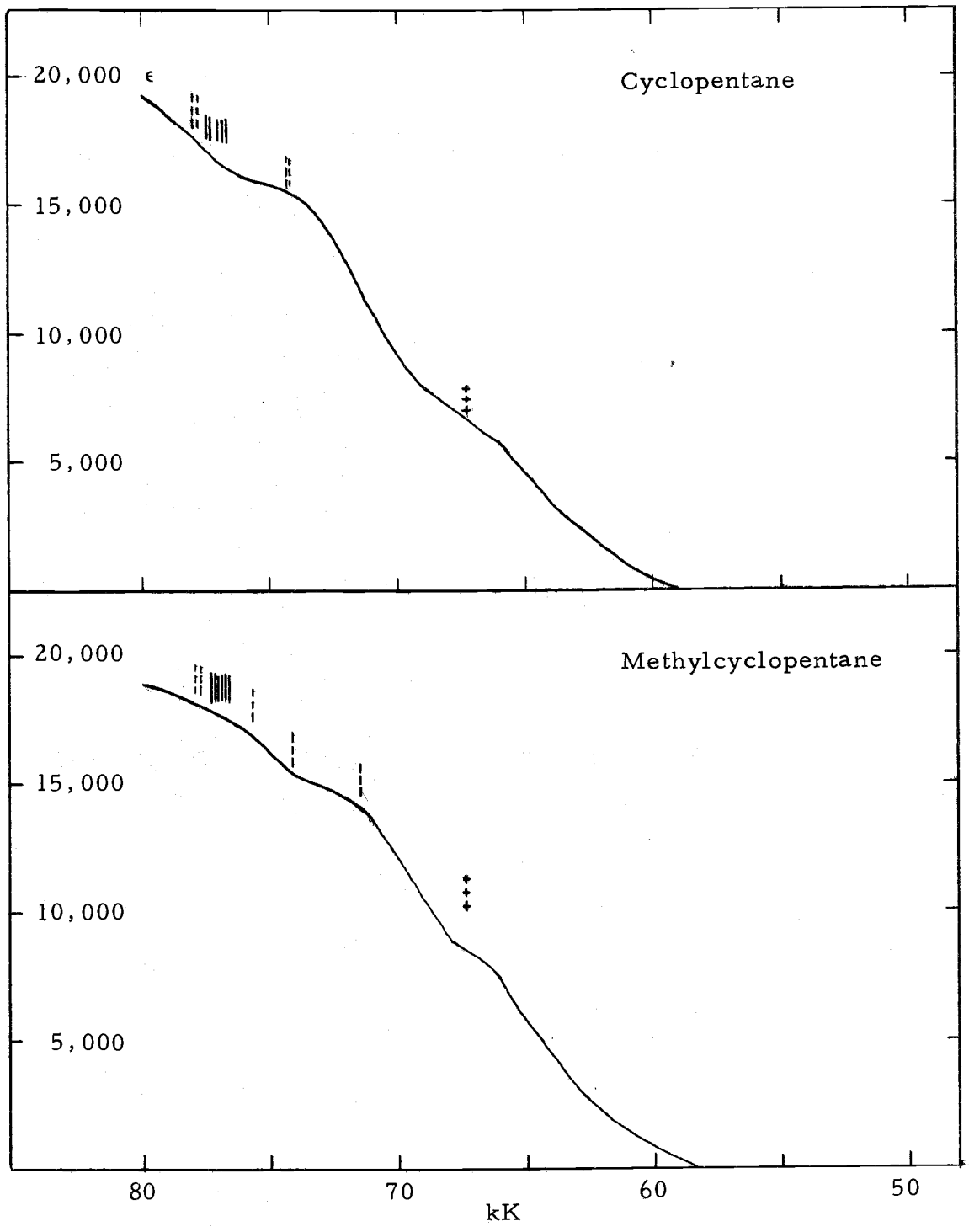

Figure 24. Spectra of cyclic alkanes with predicted peaks. Solid lines are CH bonds; dashed lines are CH and CC; crosses are CC bond transitions.

distinguish them at higher energies. Thus, we designate these by a cross hatched bar.

Thus we note that the calculated $\sigma - \sigma^*$ spectra show no transitions below 67 kK, but the experimental spectra show many transitions between 50 kK and 67 kK. We have concluded, therefore, that these low energy transitions are not caused by excitations of bonding electrons. We believe that these bands are due to the 2p nonbonding electrons on the oxygen atoms.

Nonbonding electrons may be excited either to antibonding states, called σ^*, or to higher atomic states in Rydburg transitions. This idea is discussed in some detail by Tsubomura et al. (48).

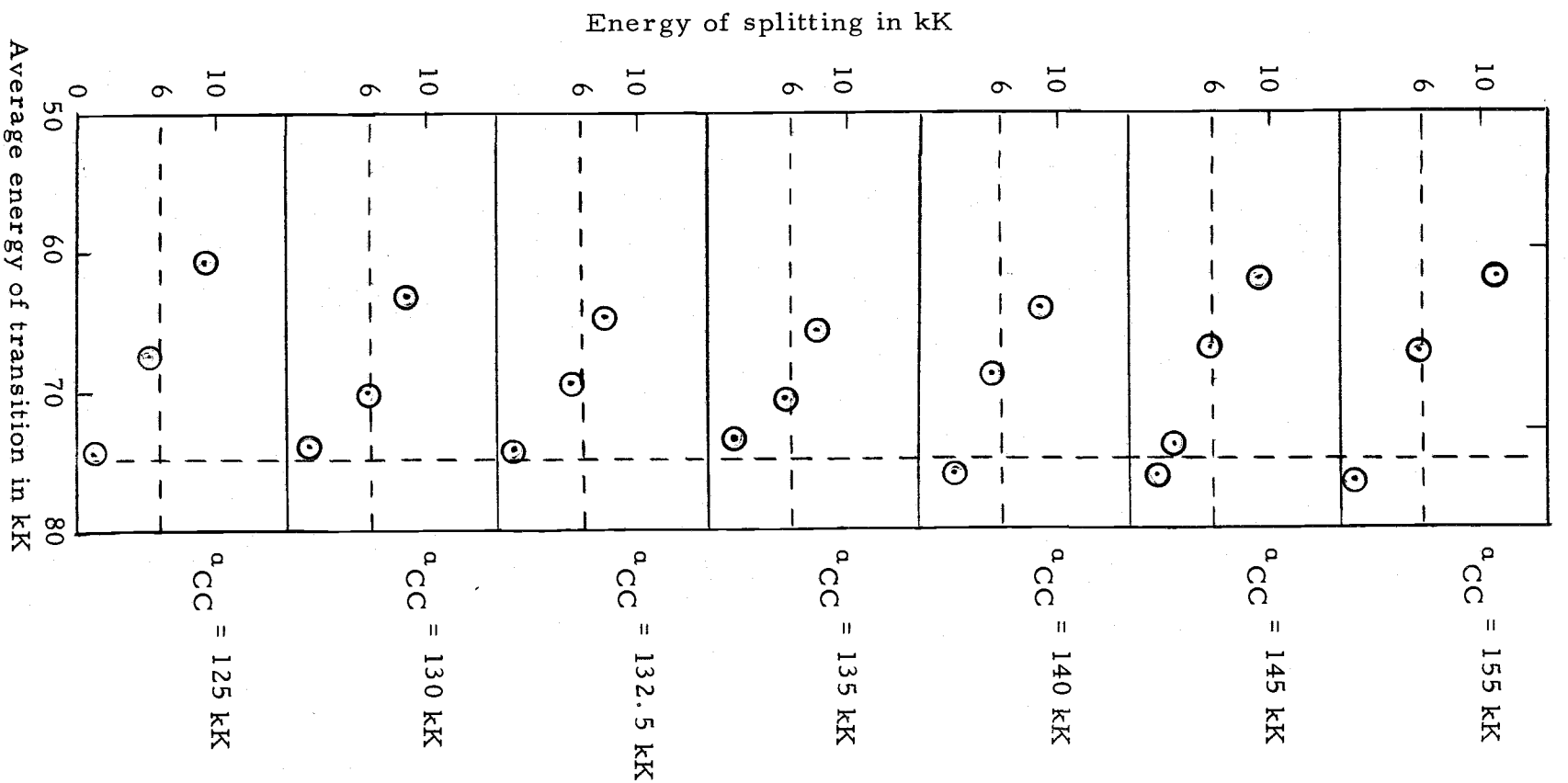

Figure 25. Energy splittings versus average transition energies in kK for propane. Calculated by independent systems. a_{CH} was always 105 kK. The vertical dashed line shows the experimental average energy. The horizontal dashed lines show the experimental splitting. Note that these dashed lines never cross in the region of the calculated points.

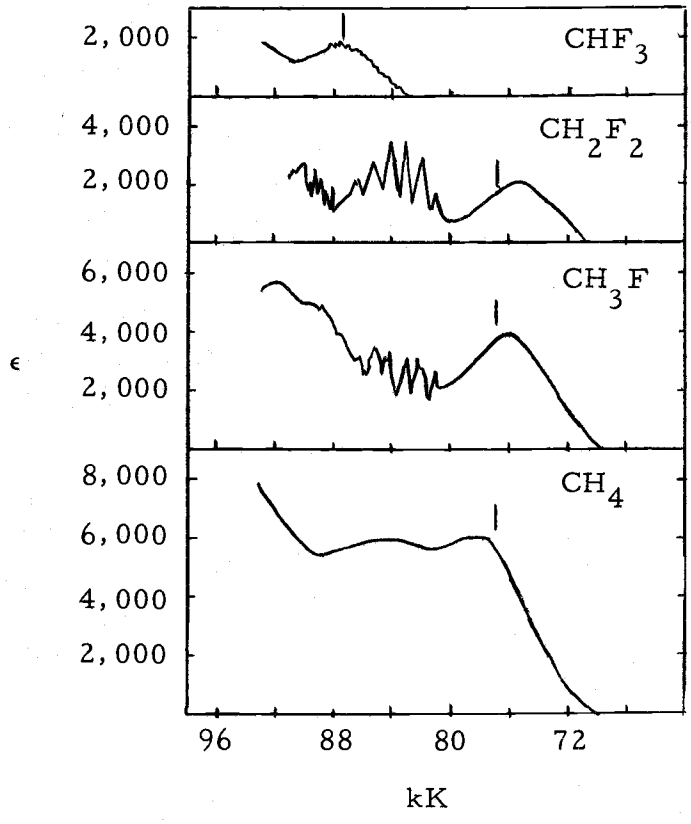

Figure 26. Observed fluoromethane spectra with predicted peaks shown as vertical lines.

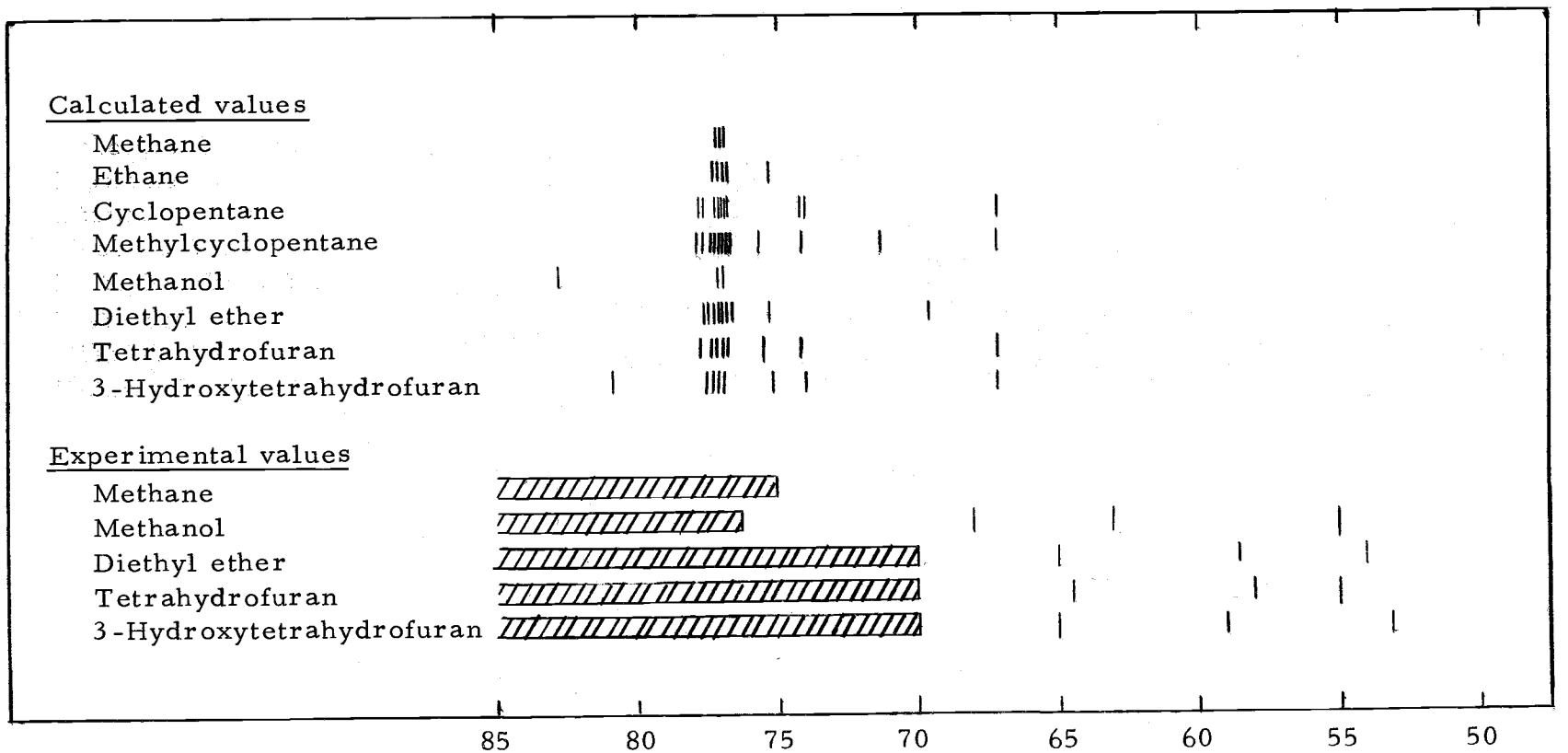

Figure 27. Comparison of results of independent systems calculation to experiment for some representative model sugars.

PREDICTION OF SPECTRA OF COMPLEX MOLECULES

Having satisfied ourselves that the lower energy transitions originate from the 2p nonbonding oxygen electrons, we now wish to show that these transitions in the simple ethers and alcohols can be combined in a logical way to produce the spectra of more complex molecules. For the compound 3-hydroxytetrahydrofuran, we demonstrate in Figure 28 that this is possible. We subtracted away the $\sigma - \sigma^*$ transitions in two alcohols (ethanol, and cyclohexanol) and two ethers (diethyl ether and tetrahydrofuran) and averaged the extinction coefficients and positions of the remaining peaks. Figure 28c shows the $\sigma - \sigma^*$ transitions of the bonding electrons. When the extinction coefficients of these spectra were simply added together at each energy point, the theoretical spectrum of 3-hydroxytetrahydrofuran was obtained as is shown below. This compared rather well to the actual experimental spectrum of the compound. Though the calculated peaks are more intense than the experimental ones, the three nonbonding peaks do fall at approximately the same energies in the two spectra.

The calculated spectrum of tetrahydrofurfuryl alcohol would be very similar to this of 3-hydroxytetrahydrofuran. Note in Figure 10 that in tetrahydrofurfuryl alcohol the same three peaks are there, but in slightly different positions. The peaks at 53 and 59 kK in

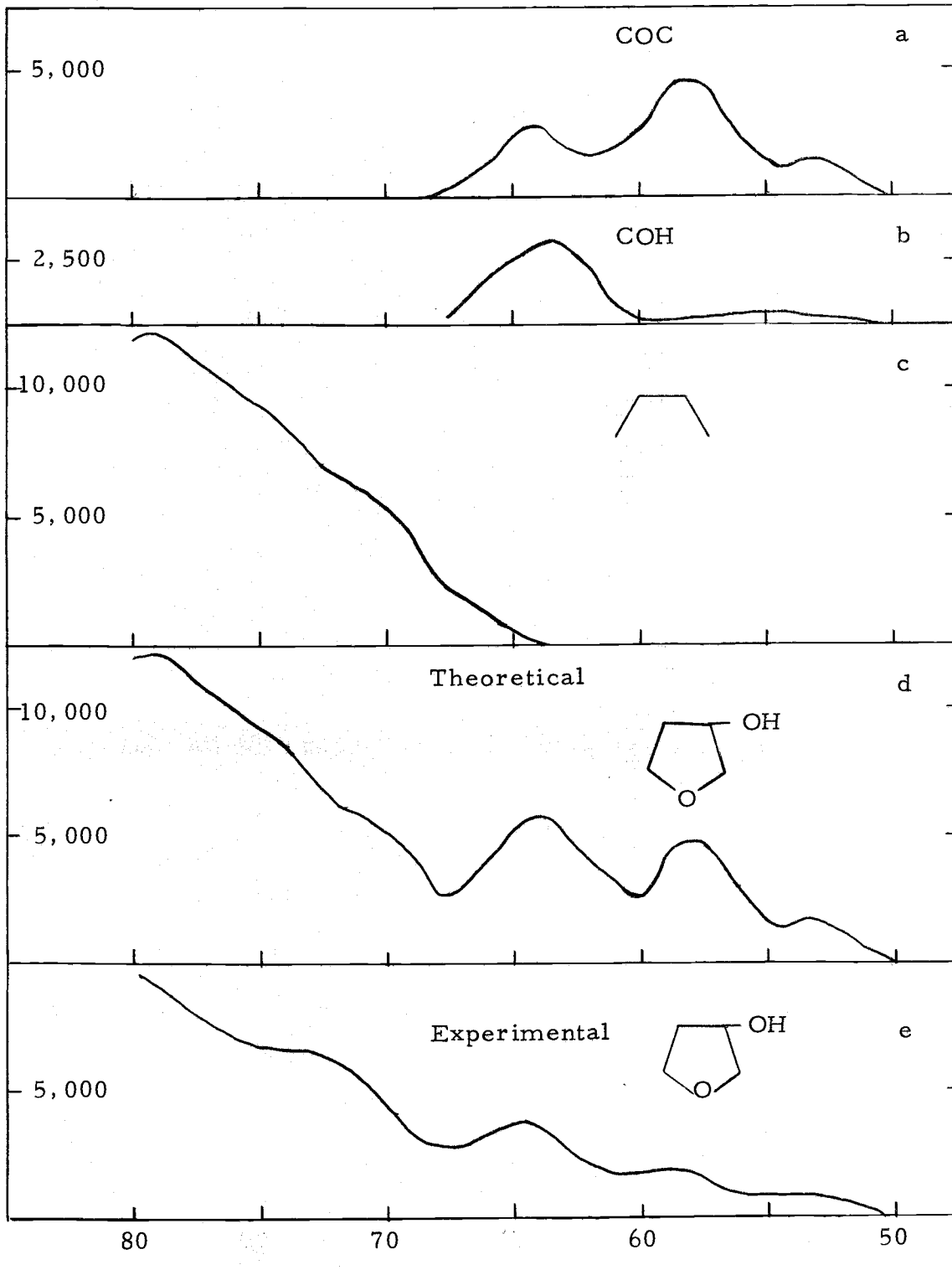

Figure 28. Prediction of spectrum of 3-hydroxytetrahydrafuran.

3-hydroxytetrahydrofuran have been blue shifted enough that they appear as shoulders in tetrahydrofurfuryl alcohol. The shifting is neither very great nor very surprising considering the differences in structure between the two compounds.

A slightly different method gave a theoretical spectrum for tetrahydropyran-2-methanol, shown in Figure 29. Tetrahydropyran (Figure 7) and 2-methyltetrahydropyran (Figure 8) both have peaks at 67 to 68 kK and at about 57 kK. We would definitely consider the lower energy peak to be a nonbonding transition. The higher energy peak is on the border line, however. It is probably also nonbonding, but we cannot state this positively. Cyclohexane has a peak at the same energy, but with twice the intensity, so it is doubtful that these peaks correspond. Thus, we did not attempt to separate the oxygen $\sigma - \sigma^*$ transitions from the $n - \sigma^*$ transitions for 2-methyltetrahydropyran. For the present purpose, the whole spectrum of 2-methyltetrahydropyran is smoothed and plotted in Figure 29b.

For the alcohol part, it was necessary to shift the higher energy peak 3 kK to the red to make the sum of the two plotted in Figure 29c resemble the experimental spectrum in Figure 29d. This higher energy peak of alcohol has been called a Rydberg transition and its position has been shown by Edwards (5) to be dependent on the ionization potential of the compound. The ionization potential of tetrahydropyran-2-methanol is not known, but it is quite likely to differ

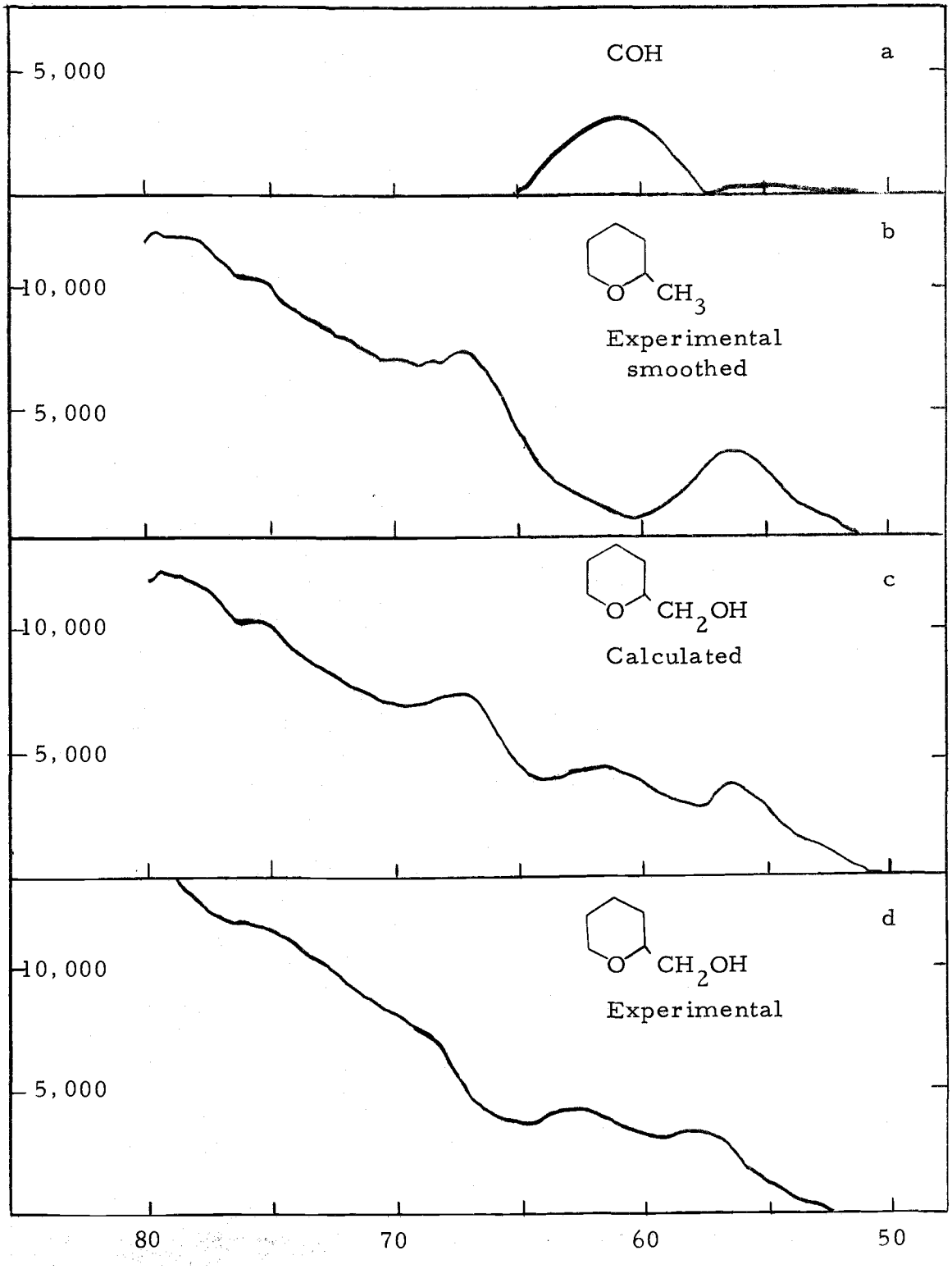

Figure 29. Prediction of spectrum for tetrahydropyran-2-methanol.

from that of ethanol. Thus, red shifting this peak is not unreasonable.

The 1,3-dioxane and 2-hydroxytetrahydropyran spectra are not as easy to analyze. In the 1,3-dioxane, there is still apparently one nonbonding transition, but it has shifted 6.5 kK to the blue as compared to tetrahydropyran. The 2-hydroxytetrahydropyran also shows only one distinct peak which is in about the same position as that in tetrahydropyran, but considerably smaller. It seems likely that the two oxygen atoms in each of these molecules are geometrically close enough together so that the nonbonding electrons are able to interact. If this were the case, the spectra would be expected to change considerably from any of the simple ethers or alcohols.

Considering that monosaccharides, or simple sugars, are made up of the same kinds of bonds present in the model compounds, we believe the low energy transitions which can be seen in absorbance and circular dichroism spectra will be interpreted in terms of transitions by the nonbonding electrons of the oxygen atoms.

The spectrum of simple D-glucose, for example, would probably have the transitions of 2-hydroxytetrahydropyran plus three hydroxyl groups and a hydroxymethyl group as in tetrahydropyran-2-methanol (see Figure 30). The $\sigma - \sigma^*$ transitions of saccharides will differ from those of the model compounds in that the saccharides have more CO and OH transitions and fewer CH transitions.

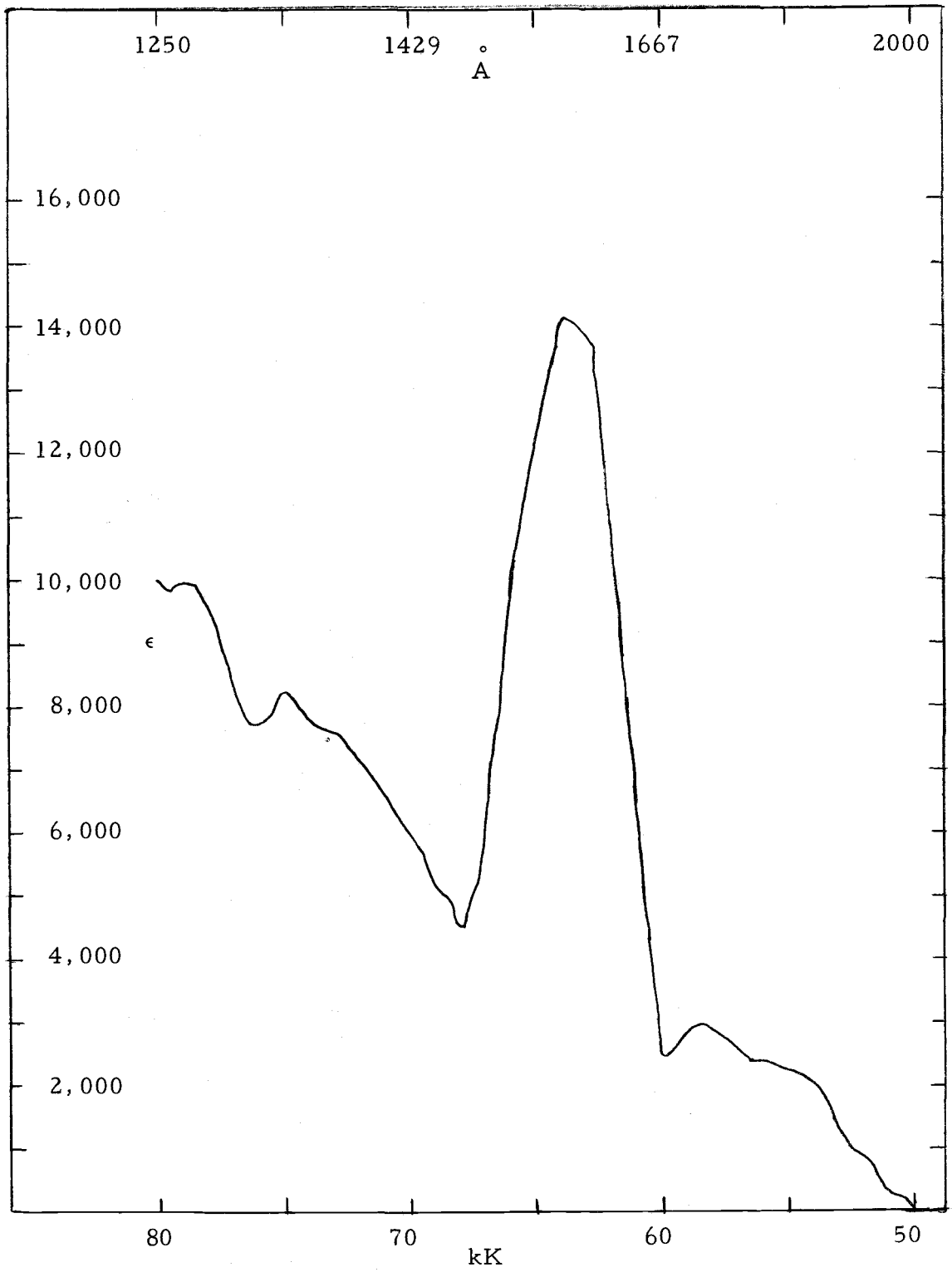

Figure 30. Predicted spectrum of glucose.

BIBLIOGRAPHY

1. Allen, Leland C. and J. Dennis Russell. Extended Huckel theory and the shape of molecules. The Journal of Chemical Physics 46:1029-1037. 1967.

2. Barnes, Edwin E. and William T. Simpson. Correlations among electronic transitions for carbonyl and for carboxyl in the vacuum ultraviolet. The Journal of Chemical Physics 39:670-675. 1963.

3. C.R.C. Handbook of chemistry and physics. 47ed. ed. by Robert C. Weast, Cleveland, Chemical Rubber Publishing Co. 1966-1967. various paging.

4. Cook, G.R. and B.K. Ching. Photoionization and absorption cross sections and fluorescence of CF_4. The Journal of Chemical Physics 43:1794-1797. 1965.

5. Edwards, Lawrence Oliver. Vacuum ultraviolet studies: I. Assignment of spectra. Doctoral dissertation. Eugene, University of Oregon. 1969. 129 numb. leaves.

6. Edwards, Lawrence and John W. Raymonda. Assignment of electronic transitions in the fluoromethanes. A bond exciton interpretation. Journal of the American Chemical Society 91:5937-5939. 1969.

7. Ellison, Frank O. and Harrison Shull. Molecular calculations. I. LCAO MO self-consistent field treatment of the ground state of H_2O. The Journal of Chemical Physics 23:2348-2357. 1955.

8. Eyring, Henry, John Walter and George E. Kimball. Quantum chemistry. New York, John Wiley, 1944. 394 p.

9. Goeppert-Mayer, M. and A.L. Sklar. Calculations of the lower excited levels of benzene. The Journal of Chemical Physics 6:645-652. 1938.

10. Harrison, Anna J., Betty J. Cederholm and Margery A. Terwilliger. Absorption of acyclic oxygen compounds in the vacuum ultraviolet. I. Alcohols. The Journal of Chemical Physics 30:355-356. 1959.

11. Harrison, Anna J. and Diana R. W. Price. Absorption of acyclic oxygen compounds in the vacuum ultraviolet. II. Ethers. The Journal of Chemical Physics 30:357-360. 1959.

12. Hernandez, G. J. Vacuum ultraviolet absorption spectrum of dimethyl ether. The Journal of Chemical Physics 38:1644-1646. 1963.

13. _____ Vacuum ultraviolet absorption spectrum of diethyl ether. The Journal of Chemical Physics 39:1355-1356. 1963.

14. _____ Vacuum ultraviolet absorption spectra of the cyclic ethers: Trimethylene oxide, tetrahydrofuran, and tetrahydropyran. The Journal of Chemical Physics 38:2233-2242. 1963.

15. Hernandez, G. J. and A. B. F. Duncan. Vacuum ultraviolet absorption spectra of 1,4-dioxane and 1,3-dioxane. The Journal of Chemical Physics 36:1504-1508. 1962.

16. Hinze, Jurgen and H. H. Jaffé. Electronegativity. I. Orbital electronegativity of neutral atoms. Journal of the American Chemical Society 84:540-546. 1961.

17. Hoffmann, Roald. An extended Huckel theory. I. Hydrocarbons. The Journal of Chemical Physics 39:1397-1412. 1963.

18. Holden, Maretta P. Graduate Research Assistant, University of Washington, Dept. of Chemistry. Unpublished spectrum of isopropanol. Seattle, Washington. 1964.

19. Klessinger, Martin. Self-consistent group calculations of polyatomic molecules. IV. Substituted methanes. The Journal of Chemical Physics 53:225-232. 1970.

20. Magnasco, Valero and G. F. Musso. A simple model of short-range interactions. II. The orientation dependence of the interaction between non-bonded hydrogen atoms. Theoretica Chimica Acta (Berlin) 21:280-286. 1971.

21. _____ Simple model of short-range interactions. III. Ethane, propane and butane. The Journal of Chemical Physics 54:2925-2935. 1971.

22. Mataga, Noboru and Kitisuke Nishimoto. Electronic structure and spectra of nitrogen heterocycles. Zeitschrift fur Physikalische Chemie Neue Folge 13:140-157. 1957.

23. McRae, E.G. and M. Kasha. Physical processes in radiation biology. New York, Academic Press, Inc., 1964. pp. 23-42.

24. Miller, James, John M. Gerhauser and F.A. Matsen. Quantum chemistry integrals and tables. Austin, University of Texas Press, 1959. various paging.

25. Mullikin, Robert S. Quelques aspects de la théorie des orbitales moléculaires. Journal de Chimie Physique 46:497-542. 1949.

26. Mullikin, Robert S. et al. Formulas and numerical tables for overlap integrals. The Journal of Chemical Physics 17:1248-1267. 1949.

27. Nelson, Richard G. and W. Curtis Johnson, Jr. Optical properties of sugars: Circular dichroism of monomers at equilibrium. Journal of the American Chemical Society. Accepted 1972.

28. Nishimoto, Kitisuke and Noboru Mataga. Electronic structure and spectra of some nitrogen heterocycles. Zeitschrift fur Physikalische Chemie Neue Folge 12:335-338. 1957.

29. Pariser, Rudolf. An improvement in the π-electron approximation in LCAO MO theory. The Journal of Chemical Physics 21:568-569. 1953.

30. Pauling, Linus. General chemistry. 3d ed. San Francisco, W.H. Freeman, 1970. 959 p.

31. Pauling, Linus. The nature of the chemical bond and the structure of molecules and crystals. 3d ed. Ithica, Cornell University Press, 1960. 644 p.

32. Pickett, Lucy W., Nancy J. Hoeflich and Tien-Chuan Liu. The vacuum ultraviolet absorption spectra of cyclic compounds. II. Tetrahydrofuran, tetrahydropyran, 1,4-dioxane and furan. Journal of the American Chemical Society 73:4865-4869. 1951.

33. Pople, J.A. Electron interaction in unsaturated hydrocarbons. Transactions of the Faraday Society 49:1375-1385. 1953.

34. Pople, J. A., D. P. Santry and G. S. Segal. Approximate self-consistent molecular orbital theory. I. Invariant procedures. The Journal of Chemical Physics 43:S129-S135. 1965.

35. Pople, J. A. and G. A. Segal. Approximate self-consistent molecular orbital theory. II. Calculations with complete neglect of differential overlap. The Journal of Chemical Physics 43:S136-S151. 1965.

36. _____ Approximate self-consistent molecular orbital theory. III. CNDO results for AB_2 and AB_3 systems. The Journal of Chemical Physics 44:3289-3296. 1966.

37. Raymonda, John Warren. Assistant Professor, University of Arizona, Dept. of Chemistry. Independent systems calculations for transition energies of alkanes. Tucson, Arizona. 1969.

38. _____ An experimental and theoretical study of sigma bond electronic transitions in alkanes. Doctoral dissertation. Seattle, University of Washington, 1966. 174 numb. leaves.

39. Rein, Robert et al. Iterative extended Huckel theory. The Journal of Chemical Physics 45:4743-4744. 1966.

40. Robin, Melvin B. and W. T. Simpson. Assignment of electronic transitions in azo dye prototypes. The Journal of Chemical Physics 36:580-588. 1962.

41. Roothaan, C. C. J. A study of two-center integrals useful in calculations on molecular structure. I. The Journal of Chemical Physics 19:1445-1458. 1951.

42. Schniepp, L. E. and H. H. Geller. Preparation of dihydropyran, δ-hydroxyvaleraldehyde and 1,5-pentanediol from tetrahydrofurfuryl alcohol. Journal of the American Chemical Society 68: 1646-1648. 1946.

43. Shimada, Ryoichi and Lionel Goodman. Polarization of aromatic carbonyl spectra. The Journal of Chemical Physics 43:2027-2041. 1965.

44. Simpson, William T. Resonance force theory of carotenoid pigments. Journal of the American Chemical Society 77:6164-6168. 1955.

45. Simpson, William T. Theories of electrons in molecules. Englewood Cliffs, Prentice Hall, 1962. 183 p.

46. Snyder, Patricia A. Research associate, Oregon State University, Dept. of Biochemistry and Biophysics. Unpublished spectrum of 2-butanol. Corvallis, Oregon. 1971.

47. Streitwieser, Andrew, Jr. Molecular orbital theory for organic chemists. New York, John Wiley, 1961. 489 p.

48. Tsubomura, Hiroshi et al. Vacuum ultraviolet absorption spectra of saturated organic compounds with non-bonding electrons. Bulletin of the Chemical Society of Japan 37:417-423. 1964.

49. Woods, G. Forrest, Jr. 5-hydroxypentanal. In: Organic syntheses, ed. by E. C. Horning (ed.-in-chief) Collective vol. 3. Rev. ed. New York, John Wiley, 1955. p. 470-471.

APPENDICES

APPENDIX I

Statement Listing of Fortran Program for Independent Systems Calculation

The first one is by the author, the subroutine is by M. S. Itzkowitz. The program requires the matrix elements above the diagonal for calculation of the eigenvalues and eigenvectors for a molecule. For calculation of the molecular transition moments and transition intensities, this program requires the vector transition moments for the isolated bonds. An example is included.

```
3/28/72
INDEPENDENT SYSTEMS CALCULATION OF ELECTRONIC
TRANSITIONS IN:
METHANE
ORDER OF ARRAY
<> 4
GIVE MATRIX ELEMENTS ABOVE DIAGONAL
<> 95.6 18.6 18.6 18.6
<> 95.6 18.6 18.6
<> 95.6 18.6
<> 95.6
WHOLE SYMMETRIC MATRIX
    95.600    18.600    18.600    18.600
    18.600    95.600    18.600    18.600
    18.600    18.600    95.600    18.600
    18.600    18.600    18.600    95.600
EIGENVALUE     77.000
EIGENVECTOR
      .707    -0.707         0         0
EIGENVALUE     77.000
EIGENVECTOR
    -0.500    -0.500      .499      .501
EIGENVALUE     77.000
EIGENVECTOR
      .001      .001    -0.708      .707
EIGENVALUE    151.400
EIGENVECTOR
      .500      .500      .500      .500
GIVE BOND VECTORS I, J, K
<>  -.5774 0 .8165
<> -.5774  .8165  0
<> -.5774 -.8165  0
<>  .5774  0  .8165
THESE ARE TRANSITION MOMENTS
          I              J              K
          0         -0.577          .577
       .578         -0.816          .001
       .816           .578          .577
    -0.577         -0.000          .816
INTENSITY IS        .667 AT       77.000
INTENSITY IS       1.000 AT       77.000
INTENSITY IS       1.333 AT       77.000
INTENSITY IS       1.000 AT      151.400
```

```
00001:       PROGRAM MATRIX
00002:       DIMENSION A(20,20), EIVU(20), EIVR(20,20)
00003:       DIMENSION B(20,3),D(20,3),DD(20)
00004:   10  CALL DATE(XDATE)
00005:       WRITE (61,13) XDATE
00006:   13  FORMAT(///// A8)
00007:       PRINT 12
00008:   12  FORMAT (' INDEPENDENT SYSTEMS CALCULATION OF ELECTRONIC')
00009:       PRINT 16
00010:   16  FORMAT (' TRANSITIONS IN:')
00011:       READ 14,I
00012:   14  FORMAT (A4)
00013:       PRINT 1
00014:   1   FORMAT (' ORDER OF ARRAY')
00015:       N=FFIN(60)
00016:       PRINT 2
00017:   2   FORMAT (' GIVE MATRIX ELEMENTS ABOVE DIAGONAL')
00018:       DO 15 I=1,N
00019:       DO 15 J=I,N
00020:   15  A(I,J)=A(J,I)=FFIN(60)
00021:       CALL EIGVV (A,EIVR,EIVU,N,0)
00022:       PRINT 17
00023:   17  FORMAT (' WHOLE SYMMETRIC MATRIX')
00024:       DO 75 I=1,N
00025:   75  PRINT 20, (A(I,J),J=1,N)
00026:   20  FORMAT (' '7F10.3)
00027:       DO 26 I=1,N
00028:   26  PRINT 27,(EIVU(I),(EIVR(K,I),K=1,N))
00029:   27  FORMAT (' EIGENVALUE ' F10.3/' EIGENVECTOR'/
00030:      C' '7F10.3/' '7F10.3/' '7F10.3/' '7F10.3)
00031:       PRINT 100
00032:  100  FORMAT ( ' GIVE BOND VECTORS I, J, K')
00033:       M=3
00034:       DO 150 K=1,N
00035:       DO 150 J=1,M
00036:  150  B(K,J)=FFIN(60)
00037:       PRINT 101
(001):   101 FORMAT (' THESE ARE TRANSITION MOMENTS'/9X,' I',
00039:      C12X,' J',12X,' K')
00040:       DO 30 I=1,N
00041:       DO 29 J=1,M
00042:       D(I,J)=0
00043:       DO 29 K=1,N
00044:   29  D(I,J)=D(I,J)+EIVR(K,I)*B(K,J)
00045:   30  PRINT 31,(D(I,J),J=1,M)
00046:   31  FORMAT  (3F14.3)
00047:       DO 41 I=1,N
00048:       DD(I)=0
00049:       DO 40 J=1,M
00050:   40  DD(I)=DD(I)+D(I,J)**2
00051:   41  PRINT 50,(DD(I),EIVU(I))
00052:   50  FORMAT(' INTENSITY IS' F14.3 ' AT' F14.3)
00053:       GO TO 10
00054:       END

]
```

```
      SUBROUTINE EIGVV(A,EIVR,EIVU,N,INDIC)                              00001
C                                                                        00002
C     M.S.ITZKOWITZ     11/27/67                                         00003
C     ADAPTED FROM PROGRAM F2 CAL JACVAT, WRITTEN BY BILL POOLE,UCB      00004
C                                                                        00005
C     THIS PROGRAM FINDS THE EIGENVALUES AND, IF DESIRED, THE EIGEN-     00006
C     VECTORS OF A REAL SYMMETRIC MATRIX, ≠A≠ OF ORDER ≠N≠.  ≠A≠, ≠EIVU≠,  00007
C     AND ≠EIVR≠ ARE DIMENSIONED ≠NDIM≠  THE JACOBI METHOD IS USED TO    00008
C     TRANSFORM THE GIVEN MATRIX INTO A DIAGONAL MATRIX.  THE METHOD     00009
C     USED IS A THRESHOLD METHOD.  THE FIRST THRESHOLD IS SET EQUAL TO   00010
C     THE ROOT MEAN SQUARE OF THE OFF-DIAGONAL ELEMENTS OF THE MATRIX .  00011
C     A TRANSFORMATION IS PERFORMED WHENEVER AN OFF-DIAGONAL             00012
C     ELEMENT IS GREATER THAN THE THRESHOLD.  THE THRESHOLD IS           00013
C     UPDATED AFTER EVERY TRANSFORMATION.  EVENTUALLY A SERIES OF        00014
C     SUCH TRANSFORMATIONS REDUCES THE GIVEN MATRIX TO A DIAGONAL MATRIX 00015
C     THE ELEMENTS OF WHICH ARE THE EIGENVALUES OF THE ORIGINAL MATRIX.  00016
C     A SIMILAR SET OF TRANSFORMATIONS APPLIED TO THE IDENTITY MATRIX    00017
C     YIELDS THE MATRIX WHOSE COLUMNS ARE THE CORRESPONDING EIGENVECTORS. 00018
C                                                                        00019
C     THE MATRIX IS ASSUMED SYMMETRIC UPON ENTRY.  NO TEST IS MADE.      00020
C     THE PROGRAM THEN SCANS THE MATRIX AND PERFORMS A ROTATION WHENEVER 00021
C     THE CHOSEN ELEMENT IS GREATER THAN OR EQUAL TO THE THRESHOLD.  THE 00022
C     PROGRAM STOPS SCANNING WHENEVER EVERY ROTATION IN A COMPLETE SCAN  00023
C     IS LESS THAN ROUND-OFF ERROR.                                      00024
C     UPON EXIT, THE EIGENVALUES ARE ORDERED ALGEBRAICALLY IN ≠EIVU≠     00025
C     AND THE CORRESPONDING COLUMNS OF ≠EIVR≠ ARE THE ORTHONORMAL EIGEN- 00026
C     VECTORS.   THE ORIGINAL MATRIX IS RESTORED.                        00027
C     ≠INDIC≠ IS USED TO DETERMINE WHETHER OR NOT THE EIGENVECTORS ARE   00028
C     WANTED.  IF IT IS ZERO, THEY ARE CALCULATED. IF NON-ZERO THEY ARE  00029
C     NOT.  ≠N≠ MUST BE LESS THAN OR EQUAL TO ≠NDIM≠.  ≠NDIM≠ MUST BE LESS 00030
C     161.  IF ≠INDIC≠ IS NON-ZERO, ≠EIVR≠ MAY BE AN UNDIMENSIONED DUMMY. 00031
C                                                                        00032
      DIMENSION A(20,20),EIVU(20),EIVR(20,20)                            00033
      IF(N.GT.160)GO TO 8000                                             00034
      IF(N.LT.1) GO TO 8001                                              00035
      IF(INDIC.NE.0) GO TO 100                                           00036
      DO 50 J=1,N                                                        00037
      DO 51 I=1,N                                                        00038
51    EIVR(I,J)=0.                                                       00039
50    EIVR(J,J)=1.0                                                      00040
C                                                                        00041
C     SEARCH FOR LARGEST ABSOLUTE MATRIX ELEMENT                         00042
C                                                                        00043
100   ATOP=0                                                             00044
      DO 112 J=1,N                                                       00045
      DO 111 I=1,J                                                       00046
      IF(ABS(A(I,J)).GT.ATOP) ATOP=ABS(A(I,J))                           00047
111   CONTINUE                                                           00048
      EIVU(J)=A(J,J)                                                     00049
112   CONTINUE                                                           00050
      IF (ATOP.EQ.0.) GO TO 8002                                         00051
      IF(N.EQ.1) RETURN                                                  00052
C                                                                        00053
C     CALCULATE THE STOPPING CRITERION, DSTOP                            00054
C                                                                        00055
      AVGF=FLOAT(N*(N-1))*0.55                                           00056
      D=0.                                                               00057
      DO 114 JJ=2,N                                                      00058
      DO 114 II=2,JJ                                                     00059
      S=A(II-1,JJ)/ATOP                                                  00060
114   D=S*S+D                                                            00061
```

```
      OSTOP=1.0E-06*D                                                   00062
C                                                                       00063
C   CALCULATE THE THRESHOLD,THRSH                                       00064
C                                                                       00065
      THRSH=SQRT(D/AVGF)*ATOP                                           00066
C                                                                       00067
C   START SWEEP THROUGH MATRIX                                          00068
C                                                                       00069
115   IFLAG=0                                                           00070
      DO 130 JCOL=2,N                                                   00071
      JCOL1=JCOL-1                                                      00072
      DO 130 IROW=1,JCOL1                                               00073
      AIJ=A(IROW,JCOL)                                                  00074
C                                                                       00075
C   COMPARE THIS ELEMENT WITH THRESHOLD                                 00076
C                                                                       00077
      IF(ABS(AIJ).LE.THRSH) GO TO 130                                   00078
      AII=A(IROW,IROW)                                                  00079
      AJJ=A(JCOL,JCOL)                                                  00080
      S=AJJ-AII                                                         00081
C                                                                       00082
C   IS PROPOSED ROTATION LESS THAN ROUND-OFF ERROR                      00083
C   IF IT IS, SKIP ROTATION                                             00084
C                                                                       00085
      IF(ABS(AIJ).LE.1.E-09*ABS(S)) GO TO 130                           00086
      IFLAG=1                                                           00087
C                                                                       00088
C   IS THE ROTATION CLOSE TO 45 DEGREES                                 00089
C   IF SO SET SINE AND COSINE EQUAL TO 1./SQRT(2.)                      00090
C                                                                       00091
      IF(1.E-10*ABS(AIJ)-ABS(S))116,119,119                             00092
119   S=0.707106781                                                     00093
      C=S                                                               00094
      GO TO 120                                                         00095
C                                                                       00096
C   SINE AND COSINE FOR ANGLE OTHER THAN 45 DEGREES                     00097
C                                                                       00098
116   T=AIJ/S                                                           00099
      S=0.25/SQRT(0.25+T*T)                                             00100
      C=SQRT(0.5+S)                                                     00101
      S=2.*T*S/C                                                        00102
C                                                                       00103
C   CALCULATE NEW ELEMENTS OF A                                         00104
C                                                                       00105
120   DO 121 I=1,IROW                                                   00106
      T=A(I,IROW)                                                       00107
      U=A(I,JCOL)                                                       00108
      A(I,IROW)=C*T-S*U                                                 00109
121   A(I,JCOL)=S*T+C*U                                                 00110
      I2=IROW+2                                                         00111
      IF(I2.GT.JCOL) GO TO 123                                          00112
      DO 122 I=I2,JCOL                                                  00113
      T=A(I-1,JCOL)                                                     00114
      U=A(IROW,I-1)                                                     00115
      A(I-1,JCOL)=S*U+C*T                                               00116
122   A(IROW,I-1)=C*U-S*T                                               00117
123   A(JCOL,JCOL)=S*AIJ+C*AJJ                                          00118
      A(IROW,IROW)=C*A(IROW,IROW)-S*(C*AIJ-S*AJJ)                       00119
      DO 124 J=JCOL,N                                                   00120
      T=A(IROW,J)                                                       00121
      U=A(JCOL,J)                                                       00122
      A(IROW,J)=C*T-S*U                                                 00123
```

```
124   A(JCOL,J)=S*T+C*U                                                  00124
C                                                                        00125
C   ROTATION COMPLETE.  DO WE DO VECTORS                                 00126
C                                                                        00127
      IF(INDIC.NE.0) GO TO 126                                           00128
      DO 125 I=1,N                                                       00129
      T=EIVR(I,IROW)                                                     00130
      EIVR(I,IROW)=C*T-EIVR(I,JCOL)*S                                    00131
125   EIVR(I,JCOL)=S*T+EIVR(I,JCOL)*C                                    00132
C                                                                        00133
C   CALCULATE NEW NORM AND COMPARE WITH DSTOP                            00134
C                                                                        00135
126   S=AIJ/ATOP                                                         00136
      D=D-S*S                                                            00137
      IF(D.GE.DSTOP) GO TO 129                                           00138
C                                                                        00139
C   RECALCULATE DSTOP AND THRSH TO DISCARD ROUNDING ERRORS               00140
C                                                                        00141
      D=0.                                                               00142
      DO 128 JJ=2,N                                                      00143
      DO 128 II=2,JJ                                                     00144
      S=A(II-1,JJ)/ATOP                                                  00145
128   D=S*S+D                                                            00146
      DSTOP=1.E-06 * D                                                   00147
129   THRSH=SQRT(D/AVGF)*ATOP                                            00148
130   CONTINUE                                                           00149
      IF(IFLAG.NE.0) GO TO 115                                           00150
C                                                                        00151
C   TERMINATION ROUTINE, RESTORE ORIGINAL MATRIX AND SET EIVU            00152
C                                                                        00153
      T=A(1,1)                                                           00154
      A(1,1)=EIVU(1)                                                     00155
      EIVU(1)=T                                                          00156
      DO 132 J=2,N                                                       00157
      T=A(J,J)                                                           00158
      A(J,J)=EIVU(J)                                                     00159
      EIVU(J)=T                                                          00160
      DO 132 I=2,J                                                       00161
132   A(I-1,J)=A(J,I-1)                                                  00162
C                                                                        00163
C   ORDER EIGENVALUES AND VECTORS ALGEBRAICALLY                          00164
C                                                                        00165
      DO 150 J=2,N                                                       00166
      JMONE=J-1                                                          00167
      EMIN=EIVU(JMONE)                                                   00168
      JMIN=JMONE                                                         00169
      DO 151 JJ=J,N                                                      00170
      IF(EIVU(JJ).GT.EMIN) GO TO 151                                     00171
      EMIN=EIVU(JJ)                                                      00172
      JMIN=JJ                                                            00173
151   CONTINUE                                                           00174
C                                                                        00175
C   NOW SWITCH MINIMUM VALUE WITH JMONE VALUE                            00176
C                                                                        00177
      IF(JMIN.EQ.JMONE) GO TO 150                                        00178
      EIVU(JMIN)=EIVU(JMONE)                                             00179
      EIVU(JMONE)=EMIN                                                   00180
      IF(INDIC.NE.0) GO TO 150                                           00181
      DO 152 I=1,N                                                       00182
      T=EIVR(I,JMONE)                                                    00183
      EIVR(I,JMONE)=EIVR(I,JMIN)                                         00184
      EIVR(I,JMIN)=T                                                     00185
```

```
152   CONTINUE                                                                  00186
150   CONTINUE                                                                  00187
      RETURN                                                                    00188
8000   PRINT 9800                                                               00189
9800  FORMAT(20H0NDIM.LT.N FOR EIGVV)                                           00190
      CALL EXIT                                                                 00191
8001  PRINT 9801                                                                00192
9801  FORMAT(51H0ORDER OF MATRIX FOR EIGVV OUTSIDE ACCEPTABLE RANGE)            00193
      CALL EXIT                                                                 00194
8002  PRINT 9802                                                                00195
9802  FORMAT(43H0MATRIX TO BE DIAGONALIZED BY EIGVV IS ZERO)                    00196
      CALL EXIT                                                                 00197
      END                                                                       00198
```

APPENDIX II

Reprint of the Paper About Fluorocarbons as Solvents

Reprinted from **APPLIED OPTICS**, Vol. 10, page 681, March 1971

Fluorocarbons as Solvents for the Vacuum Ultraviolet

H. R. Dickinson and W. C. Johnson, Jr.

Department of Biochemistry and Biophysics, Oregon State University, Corvallis, Oregon 97331.
Received 29 December 1970.

Obtaining transparent solvents for use in the vacuum ultraviolet region has been a long standing problem for spectroscopists. Of the spectroscopic reagents which have been commercially available for some time, pentane seems to be the most transparent with a cut-off (OD = 1.0) of 1900 Å in 1-cm cells and 1680 Å in 50-μ cells. Recently Goodman and co-workers[1] have used fluorinated alcohols extensively to obtain spectra of polypeptides in the vacuum ultraviolet. The most transparent of these commercially available solvents, 1,1,1,3,3,3-hexafluoroisopropanol, has a cut-off of 1630 in 50-μ cells. We wish to report transmission studies on highly transparent perfluoro alkanes that are now commercially available.

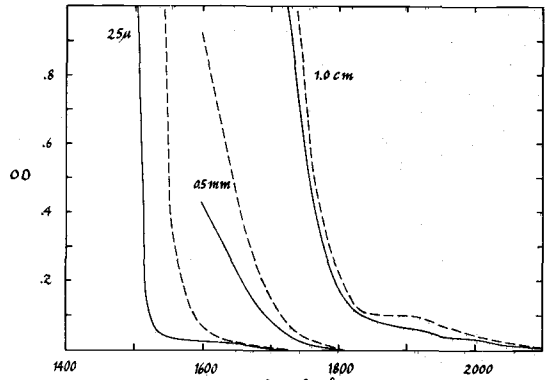

Fig. 1. The optical density of fluorocarbon solvents available from Pierce Chemical Company: ———— perfluoro *n*-hexane; ---------- perfluoro methylcyclohexane.

The idea that fluorocarbons would make suitable solvents for the vacuum ultraviolet is not new. In 1948 Klevens and Platt[2] published a paper entitled, "The Ultimate Liquid Transmission Limit?" in which they pointed out that, on the basis of refractive index and ionization potential, fluorocarbons would probably be the most transparent liquids. Perfluorinated alkanes commercially available at that time transmitted to only 1800 Å, although a repeatedly fractionated sample of perfluoro *n*-octane was transparent to 1565 Å in a 0.03-mm cell.

We have recently investigated the spectral properties of perfluoro *n*-hexane and perfluoro methylcyclohexane available from Pierce Chemical Company. Figure 1 details the spectra taken in various pathlength cells on a McPherson 225 spectrophotometer. It is interesting to note that both of these solvents were so transparent in a 0.5-mm quartz cell that they transmitted beyond the 1600-Å cut-off of the quartz itself. In a 25-μ cell with CaF_2 windows, the range of usefulness was extended to 1510 Å for perfluoro *n*-hexane and to 1540 Å for perfluoro methylcyclohexane. These transmission limits are slightly lower than Klevens and Platt[2] reported for their specially prepared perfluoro *n*-octane, and could have been predicted from the vapor phase work of Belanger *et al.*[3] and Raymonda[4] on perfluoro alkanes. From these spectra, one would expect that perfluoro *n*-pentane would be even more transparent than the solvents we investigated with a cut-off of about 1450 Å.

This work was supported by National Science Foundation Grant GB-8647. H. R. Dickinson wishes to thank the Public Health Service for an NIH traineeship. W. C. Johnson thanks the Public Health Service for Research Career Development Award GM-32784 from the NIH Institute of General Medical Sciences.

References

1. M. Goodman and I. Rosen, Biopolymers **2**, 537 (1964).
2. H. B. Klevens and J. R. Platt, J. Chem. Phys. **16**, 1168 (1948).
3. G. Belanger, P. Sauvageau, and C. Sandorfy, Chem. Phys. Lett. **3**, 649 (1969).
4. J. W. Raymonda, Doctoral Dissertation, University of Washington, 1966.